International Journal of
Molecular Sciences

MDPI

Review

Impact of Hydrogen Sulfide on Mitochondrial and Bacterial Bioenergetics

Vitaliy B. Borisov [1,*] and Elena Forte [2]

[1] Belozersky Institute of Physico-Chemical Biology, Lomonosov Moscow State University, Leninskie Gory, 119991 Moscow, Russia
[2] Department of Biochemical Sciences, Sapienza University of Rome, 00185 Rome, Italy; elena.forte@uniroma1.it
* Correspondence: viborborbor@yahoo.com

Abstract: This review focuses on the effects of hydrogen sulfide (H_2S) on the unique bioenergetic molecular machines in mitochondria and bacteria—the protein complexes of electron transport chains and associated enzymes. H_2S, along with nitric oxide and carbon monoxide, belongs to the class of endogenous gaseous signaling molecules. This compound plays critical roles in physiology and pathophysiology. Enzymes implicated in H_2S metabolism and physiological actions are promising targets for novel pharmaceutical agents. The biological effects of H_2S are biphasic, changing from cytoprotection to cytotoxicity through increasing the compound concentration. In mammals, H_2S enhances the activity of F_oF_1-ATP (adenosine triphosphate) synthase and lactate dehydrogenase via their *S*-sulfhydration, thereby stimulating mitochondrial electron transport. H_2S serves as an electron donor for the mitochondrial respiratory chain via sulfide quinone oxidoreductase and cytochrome *c* oxidase at low H_2S levels. The latter enzyme is inhibited by high H_2S concentrations, resulting in the reversible inhibition of electron transport and ATP production in mitochondria. In the branched respiratory chain of *Escherichia coli*, H_2S inhibits the bo_3 terminal oxidase but does not affect the alternative *bd*-type oxidases. Thus, in *E. coli* and presumably other bacteria, cytochrome *bd* permits respiration and cell growth in H_2S-rich environments. A complete picture of the impact of H_2S on bioenergetics is lacking, but this field is fast-moving, and active ongoing research on this topic will likely shed light on additional, yet unknown biological effects.

Keywords: hydrogen sulfide; donors; gasotransmitters; molecular bioenergetics; inhibition; electron transport chain

Citation: Borisov, V.B.; Forte, E. Impact of Hydrogen Sulfide on Mitochondrial and Bacterial Bioenergetics. *Int. J. Mol. Sci.* **2021**, *22*, 12688. https://doi.org/10.3390/ijms222312688

Academic Editors: Marcin Magierowski and Binghe Wang

Received: 12 October 2021
Accepted: 22 November 2021
Published: 24 November 2021

1. Introduction

For a long time, hydrogen sulfide (H_2S) had been considered merely as a highly toxic and occasionally lethal gas. However, it was discovered that in mammals H_2S has physiological relevance and is endogenously generated [1,2]. Currently, H_2S is considered to be a member of the class of gasotransmitters or, in other words, endogenous gaseous signaling molecules, along with nitric oxide and carbon monoxide [3–7]. Although still debated, cyanide has also recently been proposed to be part of this class [7,8]. H_2S contributes to the regulation of important physiological processes in the cardiovascular, gastrointestinal, nervous, and respiratory systems. It shows various physiological effects in mammalian cells, but in a biphasic, concentration-dependent manner. At low, nanomolar concentrations, H_2S exhibits cytoprotective effects. At higher levels the compound induces cytotoxicity. For instance, H_2S exerts vasorelaxant effects through the opening of K_{ATP} (adenosine triphosphate) channels in vascular smooth muscle cells [9]. It also functions as a neuromodulator in the brain [1] and serves as a stimulator of angiogenesis [10]. At concentrations of 200 μM and higher, H_2S induces apoptosis of aorta smooth muscle cells through the activation of mitogen-activated protein kinases and caspase-3 [11]. In mammalian systems, H_2S is

proposed to signal via four different mechanisms: (i) serving as an antioxidant that detoxifies reactive oxygen species (ROS) and/or reactive nitrogen species (RNS); (ii) blocking and/or reducing metal active sites in metalloproteins, e.g., heme Fe sites in heme proteins; (iii) performing protein *S*-persulfidation, also known as *S*-sulfhydration (post-translational modification of a cysteine residue by adding a thiol group); (iv) performing the chemical reduction of disulfide bonds in proteins (see [12,13] and references therein) (Figure 1).

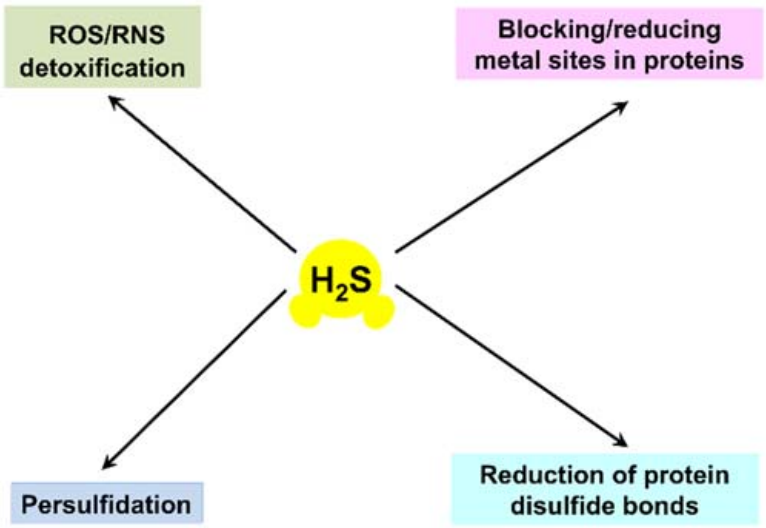

Figure 1. Proposed H_2S signaling mechanisms in mammalian systems.

The physiological roles of H_2S are not limited to mammals but appear to be inherent in all kingdoms of life. In higher plants, H_2S signaling functions seem to occur mainly through a persulfidation-based mechanism [14]. It regulates important physiological functions, including fruit ripening; stomatal movement; senescence in flowers, leaves, and fruits; photosynthesis via promotion of photosynthetic enzyme expression and chloroplast biogenesis; and the promotion of root organogenesis, seed germination, nodulation, and N_2 fixation. H_2S can also activate antioxidant systems in plant cells, thereby contributing to defense against adverse environment situations, such as drought-induced oxidative stress, salinity stress, temperature stress (high and low temperatures), toxic heavy metal stress, as well as different biotic stresses (see [14] and references therein).

Although most bacteria can generate and sense H_2S, the exact physiological roles of this compound in the prokaryotes are not yet wholly understood. In particular, whether endogenous H_2S is a true signaling effector molecule that induces a response in the same microbial cell, or whether the H_2S-mediated effect is more a response to environmental and/or host-derived H_2S, remains to be established [6]. Meanwhile, Shatalin et al. reported that inhibition of H_2S production through inactivation of H_2S-generating enzymes in *Bacillus anthracis* Sterne, *Pseudomonas aeruginosa* PA14, *Staphylococcus aureus* (MSSA RN4220 and MRSA MW2), and *Escherichia coli* MG1655 makes these pathogenic species very sensitive to different classes of antibiotics [15]. The addition of exogenous H_2S reverses this effect. The authors concluded that endogenously generated H_2S increases bacterial resistance to oxidative stress imposed by antibiotics. The antibiotic-induced ROS cause DNA damage via the Fenton reaction. It is suggested that H_2S prevents oxidative DNA damage in bacteria via the following cytoprotective mechanisms: (i) direct reduction of H_2O_2 into H_2O; (ii) depletion of Fe^{2+}, a catalyst of the Fenton reaction; (iii) transient depletion of free cysteine, a reducing agent that fuels the Fenton reaction; and (iv) stimulation of the activities of superoxide dismutase (SOD) and catalase [15]. The latter two enzymes are the well-known ROS scavenging systems [16]. It should be noted, however, that Shatalin et al. [15] did not suggest a mechanism for the depletion of Fe^{2+} and free cysteine by H_2S.

H_2S is a colorless flammable gas, soluble in water (100 mM at 25 °C [17]), and with high cell membrane permeability [18]. It is a weak acid; therefore in aqueous solutions, it equilibrates with hydrosulfide (HS^-) and sulfide (S^{2-}) according to Equation (1):

$$H_2S \overset{pK_{a1}}{\Longleftrightarrow} HS^- + H^+ \overset{pK_{a2}}{\Longleftrightarrow} S^{2-} + 2H^+ \quad (1)$$

According to the reported pK_{a1} values that varied from 6.97 to 7.06 at 25 °C (see [19] and references therein), at physiological pH 7.4, 69–73% of the total hydrogen sulfide pool in the solution is in the form of HS^-, and 27–31% exists as H_2S. Taking into account the reported pK_{a2} values (from 12.2 to 19), the concentration of S^{2-} in the solution at pH 7.4 is negligible. The mitochondrial matrix in eukaryotic cells is usually alkaline, with a pH value of about 8 [20,21]. Accordingly, in the matrix, the concentration of HS^- is higher, 90–91%, and the remainder is in the form of H_2S. On the contrary, intralysosomal pH in living cells is highly acidic, 4.7–4.8 [22]. Therefore, inside lysosomes, the undissociated form of hydrogen sulfide, H_2S, dominates (>99%). H_2S acts as a reducing agent. Respectively, the standard redox potential (vs. the standard hydrogen electrode, pH 7) $E^{0\prime}(S^0/H_2S)$ is −230 mV ($E^{0\prime}(S^0/HS^-)$ = −270 mV) [19]. Herein, unless otherwise stated, we use the term "H_2S" to designate the total hydrogen sulfide pool ($H_2S + HS^- + S^{2-}$).

This review focuses on the effects of H_2S on the respiratory chains of mammalian mitochondria and bacteria, mammalian F_oF_1-ATP synthase, and mammalian lactate dehydrogenase (LDH) in light of recent findings.

2. Endogenous Production of H_2S

In mammalian tissues, H_2S can be endogenously produced via both non-enzymatic and enzymatic pathways.

2.1. Non-Enzymatic Production of H_2S

Non-enzymatic formation of H_2S usually takes place in the reactions of thiols or thiol derivatives with other molecules [12,13,23]. Inorganic polysulfides, persulfides, and thiosulfate can be reduced with reduced glutathione (GSH) to yield H_2S (Figure 2). This demands the presence of reducing equivalents, such as NADPH (reduced nicotinamide adenine dinucleotide phosphate), because glutathione disulfide (GSSG), also produced in the reaction, needs to be converted back to GSH by NADPH-dependent glutathione reductase. Inorganic sulfide salts, such as Na_2S or NaHS, can undergo hydrolysis. Yang et al. also reported that cysteine is the preferred substrate for the non-enzymatic pathway, and that the reaction required coordinated catalysis by Fe^{3+} and pyridoxal phosphate (PLP) [24] (Figure 2).

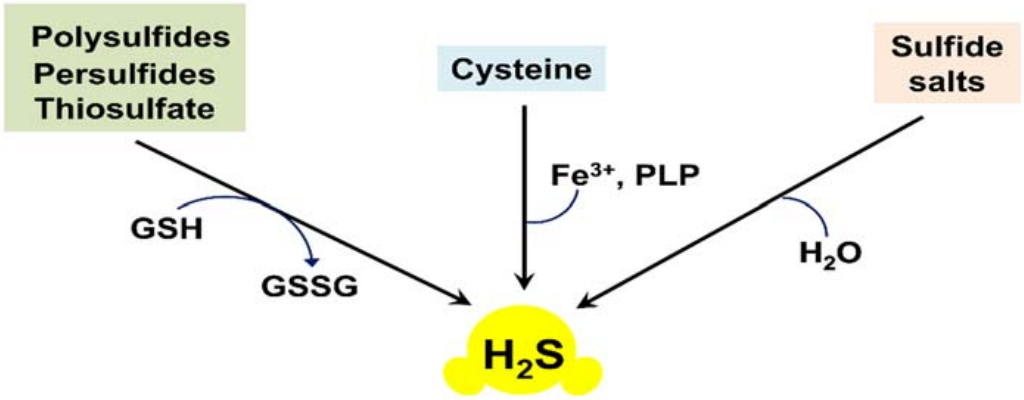

Figure 2. Non-enzymatic endogenous production of H_2S in mammalian tissues.

2.2. Enzymatic Production of H_2S

Enzymatic production of H_2S in mammalian systems is carried out primarily by cystathionine-β-synthase (CBS), cystathionine-γ-lyase (CSE), and 3-mercaptopyruvate-sulfurtransferase (3MST) [12,13,23,25,26]. The main enzymatic reactions resulting in the biosynthesis of H_2S are shown in Figure 3. CBS can catalyze the condensation of homocysteine and L-cysteine to produce L-cystathionine and H_2S (Figure 3, reaction 1). In the presence of L-cysteine, CBS can also produce H_2S, with the formation of L-serine as a byproduct (Figure 3, reaction 2). CSE can decompose homocysteine to yield H_2S, α-ketobutyrate, and ammonia (Figure 3, reaction 3). Furthermore, CSE can catalyze the conversion of L-cysteine into H_2S, pyruvate, and ammonia (Figure 3, reaction 4). Both CBS and CSE can generate H_2S through β-replacement of cysteine by a second cysteine, with the formation of lanthionine as a byproduct (Figure 3, reaction 5). Additionally, CSE can catalyze the γ-replacement reaction between two homocysteine molecules, with the production of H_2S and homolanthionine as a by-product (Figure 3, reaction 6). 3MST generates H_2S from 3-mercaptopyruvate coupled with either of the two enzymes, mitochondrial cysteine aminotransferase (CAT) or peroxisomal D-amino acid oxidase (DAO). 3MST transfers a sulfur atom from 3-mercaptopyruvate onto itself, resulting in the formation of the enzyme-bound persulfide (3MST-SS) and pyruvate (Figure 3, reaction 7). H_2S is then released from the persulfide in the presence of a reductant, e.g., thioredoxin (Trx). CAT and DAO in turn produce 3-mercaptopyruvate from L-cysteine and D-cysteine, respectively [13].

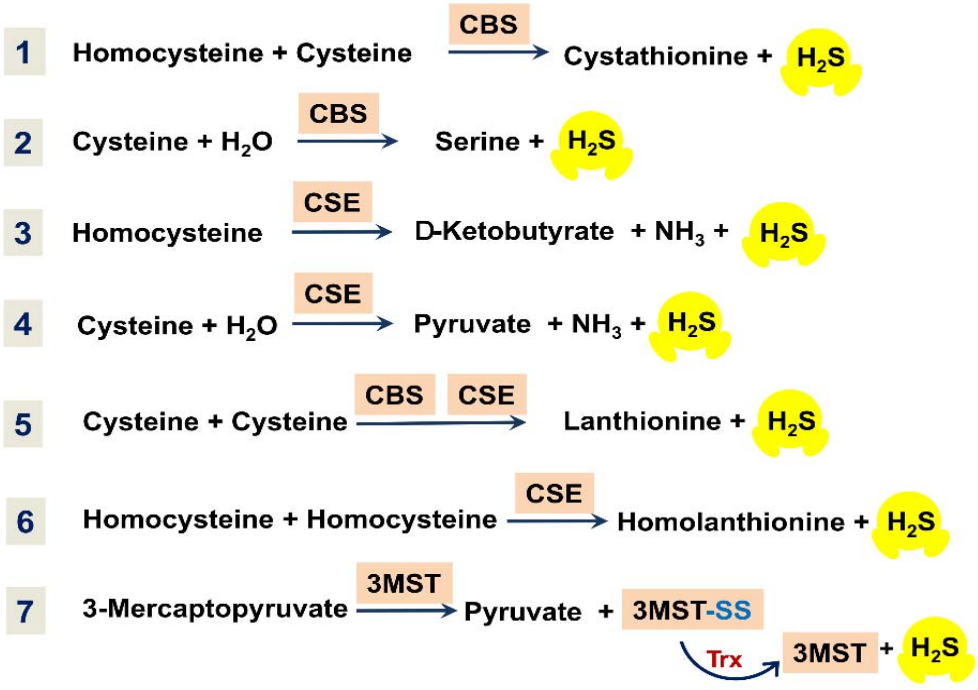

Figure 3. Overview of main reactions for enzymatic production of H_2S in mammalian tissues.

The majority of bacterial species whose genomes were completely sequenced have the orthologs of mammalian genes encoding CBS, CSE, or 3MST [15]. Since H_2S provides defense against modern antibiotics in bacteria, suppression of H_2S-producing enzymes in pathogens by new drugs would be a promising antimicrobial treatment strategy [15,27]. The use of H_2S biogenesis as a target for versatile antibiotic potentiators may have therapeutic potential for the fight against difficult-to-treat infections based on bacterial antibiotic tolerance.

3. *S*-Sulfhydration of ATP Synthase

In eukaryotes, one of the main targets of H_2S signaling is the mitochondria. These cell organelles are known to be the power plants of the eukaryotic cell. Energy transduction events in mitochondria occur in the O_2-dependent respiratory electron transport chain. The mammalian respiratory chain is unbranched [28,29]. It consists of four membrane-bound multi-subunit complexes: I, (reduced nicotinamide adenine dinucleotide) NADH: ubiquinone reductase or type I NADH dehydrogenase; II, succinate dehydrogenase; III, ubiquinol: cytochrome *c* reductase or cytochrome bc_1 complex; and IV, cytochrome *c* oxidase or cytochrome aa_3. The chain transfers electrons from NADH and succinate to O_2. The electron transfer reactions catalyzed by complexes I, III, and IV are coupled to the generation of the proton motive force. The latter is used by ATP synthase (F_oF_1-ATP synthase or complex V) to produce ATP.

Modis et al. observed *S*-sulfhydration of subunit α of the synthase (ATP5A1) in HepG2 and HEK293 cell lysates in response to exposure to H_2S, using a biotin switch assay [30]. Sulfhydration of subunit α of the synthase increases with increasing the H_2S concentration, 50–300 μM. H_2S at low concentrations (10–100 nM) stimulates the specific activity of ATP synthase, while at higher concentrations (1–10 μM) a tendency for inhibition of the activity is detected (Figure 4). Such a bell-shaped concentration–response curve is quite typical for the effects of H_2S. Sulfhydration occurs at two highly conserved cysteine residues in subunit α of the synthase, Cys244, or Cys294. Mutation of either of the two cysteines (C244S or C294S) leads to a slight reduction in the catalytic activity of ATP synthase. The double mutant (C244S/C294S) exhibits more than 50% inhibition of the enzyme activity. In vivo, subunit α of the synthase is basally sulfhydrated. The basal sulfhydration is mostly due to CSE-derived endogenous H_2S generation because it is suppressed in liver homogenates harvested from $CSE^{-/-}$ mice. Burn injuries that upregulate CSE and increase H_2S generation result in an increase in *S*-sulfhydration of subunit α of the synthase. Thus, *S*-sulfhydration of subunit α of the synthase could be a physiological mechanism to maintain ATP synthase in a physiologically activated state, thereby supporting mitochondrial bioenergetics [30].

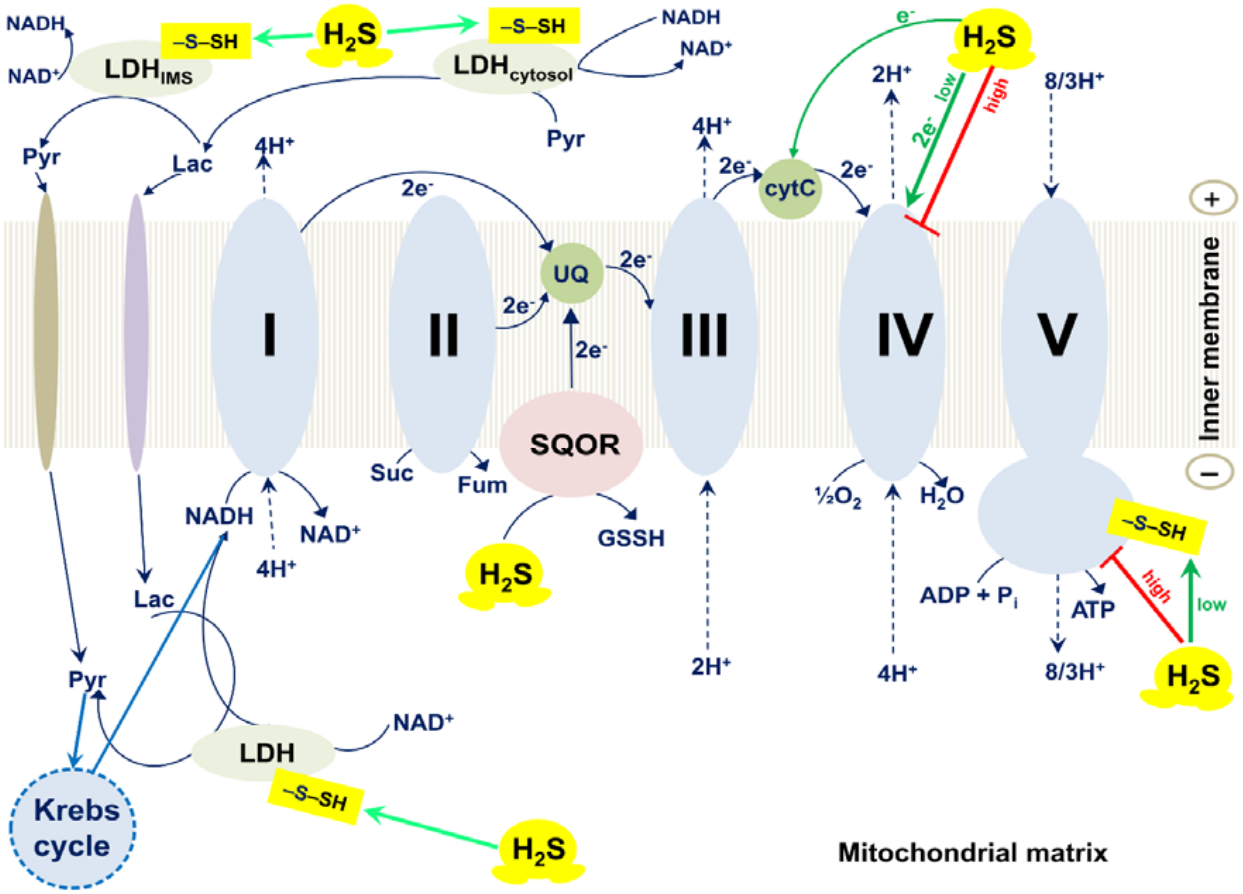

Figure 4. Effects of H_2S on mammalian mitochondrial electron transport chain, ATP synthase, and lactate dehydrogenase. The mammalian respiratory chain includes four different membrane-bound complexes: I, II, III, and IV. H_2S at low concentrations stimulates the activity of F_oF_1-ATP synthase (also known as complex V) via *S*-sulfhydration of Cys244 or Cys294 of its α subunit [30]. H_2S increases the activity of lactate dehydrogenase (LDH) via *S*-sulfhydration of its Cys163 that, in turn, stimulates mitochondrial electron transport [31]. H_2S can also donate electrons to the respiratory chain via sulfide quinone oxidoreductase (SQOR) by directly reducing ubiquinone (UQ) [32]. At high (toxic) concentrations H_2S inhibits complex IV (cytochrome *c* oxidase) and F_oF_1-ATP synthase that leads to reversible inhibition of mitochondrial electron transport and ATP production [30,33–35]. At low concentrations H_2S serves as an electron donor for complex IV, either directly [36–38] or indirectly, via reduction of its native substrate cytochrome *c* [39]. The outer mitochondrial membrane is not shown for simplicity.

4. *S*-Sulfhydration of Lactate Dehydrogenase (LDH)

LDH catalyzes the reversible conversion of lactate to pyruvate with the reduction of NAD^+ to NADH, and vice versa. The enzyme is a tetramer that is usually composed of the two most common types of subunits, LDHA and LDHB [40]. LDHA and LDHB can assemble into five different isoenzymes: LDH1, LDH2, LDH3, LDH4, and LDH5. Isoenzymes that are rich in LDHA catabolize pyruvate to lactate with the concomitant production of NAD^+ from NADH. Conversely, isoenzymes rich in LDHB facilitate lactate-to-pyruvate conversion with the concomitant formation of NADH from NAD^+.

Untereiner et al. reported that in the colon cancer cell line HCT116, LDHA catalyzes the conversion of pyruvate to lactate, and H_2S donation increases the total cellular lactate levels [31]. Notably, H_2S enhances the catalytic activity of LDHA, which is primary cytosolic, doing so via *S*-sulfhydration of its Cys163 (Figure 4). Experiments with whole HCT116 cell extracts showed that H_2S also stimulates the LDHB activity, although to a smaller extent. Importantly, H_2S stimulates oxidative phosphorylation in HCT116 cells in an LDHA-dependent manner. Thus, in colon cancer cells, H_2S-induced stimulation of the catalytic activity of LDHA leads to the stimulation of mitochondrial electron transport.

The authors hypothesize that the increase in the LDHA activity causes an increase in cytosolic lactate. This enhances the flux of lactate into the mitochondria through the intracellular lactate shuttle. Lactate enters the mitochondrial intermembrane space. Lactate and pyruvate also enter the mitochondrial matrix. Lactate is converted to pyruvate via the mitochondrial LDH that is primarily made up of LDHB and also activated by H_2S. Pyruvate in the matrix is oxidized via the Krebs cycle to generate NADH that stimulates the activity of the mitochondrial respiratory chain. Additionally, the oxidation of lactate to pyruvate by the mitochondrial LDH is coupled to the reduction of NAD^+ to NADH. This NADH, in turn, is utilized by the mitochondrial respiratory chain to further support electron transport.

5. H_2S Donates Electrons to the Mitochondrial Respiratory Chain via Sulfide Quinone Oxidoreductase (SQOR)

Powell and Somero first reported that the oxidation of H_2S can occur in mitochondria, and that the process is coupled to oxidative phosphorylation [41]. The mitochondrial oxidation of H_2S was observed in the gill and foot tissue of *Solemya reidi*, a gutless clam living in sulfide-rich habitats. Later, Goubern et al., using permeabilized human colon adenocarcinoma HT29 cells, showed that H_2S at low micromolar concentrations can serve as an electron donor for the mammalian respiratory chain [32]. This is accompanied by mitochondrial energization. The latter is extremely sensitive to the amount of H_2S delivered instantaneously to mitochondria. H_2S donates electrons at the respiratory chain at the level of UQ.

The enzyme that catalyzes the electron transfer from H_2S to UQ is SQOR [42]. SQOR belongs to group four of the flavin disulfide reductase (FDR) superfamily. The enzyme contains a tightly bound FAD (flavin adenine dinucleotide) and two spatially proximal redox-active cysteines. A peculiar feature of human SQOR is the fact that the two cysteines are linked via a bridging sulfur atom which forms the redox-active cysteine trisulfide configuration. The trisulfide appears to be the active form of SQOR, being present at the start and end of the catalytic cycle [43].

When H_2S is oxidized in the mitochondrial matrix by the action of SQOR under physiological conditions, GSH serves as the primary sulfur acceptor (Figure 4). In the reaction that is coupled to the reduction of UQ to UQH_2, glutathione persulfide (GSSH) is produced. GSSH is then oxidized by persulfide dioxygenase (ETHE1) to yield sulfite (SO_3^{2-}) and regenerate GSH. GSSH can also be a substrate for rhodanese or thiosulfate sulfurtransferase (TST). TST catalyzes the reaction of GSSH with SO_3^{2-} to generate GSH and thiosulfate ($S_2O_3^{2-}$). Alternatively, SO_3^{2-} can be oxidized to sulfate (SO_4^{2-}) by sulfite oxidase (SUOX) located in the intermembrane space, with the concomitant reduction of cytochrome *c*. Thiosulfate and sulfate can be excreted with urine (see [42] and references therein). Thus, electrons from the sulfide oxidation pathway can enter the mitochondrial respiratory chain at the level of the cytochrome bc_1 complex (from SQOR) and cytochrome *c* oxidase (from SUOX).

6. H_2S at Toxic Concentrations Inhibits Mitochondrial Cytochrome *c* Oxidase

H_2S exposure, at high concentrations and high rates, is extremely toxic to mammals, including humans [35]. The acute toxicity of H_2S is generally attributed to the suppression of the mitochondrial cytochrome *c* oxidase (complex IV). Complex IV couples the transfer of electrons from cytochrome *c* to O_2 with the generation of the transmembrane proton gradient using the mechanism of proton pumping [16,44–65]. The enzyme carries four redox-active metal sites: Cu_A, heme *a*, heme a_3, and Cu_B. Electrons from cytochrome *c* primarily accepted by Cu_A are transferred to heme *a* and then to the catalytic binuclear center composed of heme a_3 and Cu_B in which the reduction of oxygen to water occurs [66–69]. There are two forms of cytochrome *c* oxidase: slow (resting oxidase as obtained from the preparation) and fast (the completely reduced enzyme exposed to a "pulse" of O_2) [70]. The fast form is also called pulsed or unrelaxed. The slow form differs from the fast form in lower reactivity for inhibitors [71] and slower intramolecular electron transfer [72].

H_2S at high concentrations was reported to inhibit the O_2 consumption by the beef heart cytochrome *c* oxidase in the isolated form and in submitochondrial particles (Figure 4) [33,34,73]. The inhibition by H_2S appears to be non-competitive with respect to both substrates, cytochrome *c* and O_2 [34]. The inhibition efficiency increases with decreasing pH: the K_i values measured at pH 8.05, 7.48, and 6.28, are 2.6, 0.55, and 0.07 μM, respectively [37]. The initial rate of inactivation of the fast form of the isolated cytochrome *c* oxidase is proportional to total H_2S concentration, with an initial rate constant, k_{on}, of 2.2×10^4 M^{-1} s^{-1} at pH 7.47 [38]. The inhibition of complex IV leads to blockage of the mitochondrial respiratory chain and, as a consequence, to the dissipation of the membrane potential, the cessation of oxidative phosphorylation, and enhanced ROS production [35]. Consistently, examination of the cytotoxic effects of inhalational H_2S exposure showed that sublethal (>50 ppm) concentrations of the inhaled gas caused inhibition of cytochrome *c* oxidase activity in the lung and heart, which can be observed ex vivo and is associated with pathological alterations [74–79]. That complex IV is suppressed by high (usually 10–100 μM) concentrations of H_2S in vitro in various cell lines is well documented [75,80–85]. The H_2S-induced inhibition is reversible, e.g., 10–30 min after the exposure of tissue homogenates to H_2S, the activity of complex IV gets back to its initial level, simultaneously with the decomposition of the inhibitor [86].

H_2S, presumably in the form of HS^-, binds to the ferric heme a_3 and Cu_B in either state (either cupric or cuprous) [38]. The final enzyme product of H_2S inhibition is a mixed-valence state of the oxidase in which Cu_A and heme *a* are reduced and heme a_3 is in the ferric H_2S-bound form [33,87]. Cu_B in the final inhibited enzyme remains reduced even after reoxidation of the H_2S-bound oxidase, as evidenced by an electron paramagnetic resonance spectroscopy study [88]. The fact that Cu_B remains cuprous in the presence of ferricyanide suggests that H_2S binding to Cu_B^{1+} increases its redox potential and makes re-oxidation difficult. In other words, Cu_B^{1+} in this state may also be H_2S-bound [88]. Nicholls et al. [38] suggested a model for the H_2S-mediated inhibition of the mitochondrial cytochrome *c* oxidase (Figure 5). According to this model, during the steady-state turnover of complex IV, the first molecule of HS^- transiently binds to cupric or cuprous Cu_B. Then, it is transferred to the ferric heme a_3 that blocks the catalytic reaction of the heme with O_2. In the final protein-inhibitor adduct, Cu_B is likely reduced and presumably bound to the second molecule of HS^-. Heme *a* and Cu_A are most likely reduced in the adduct.

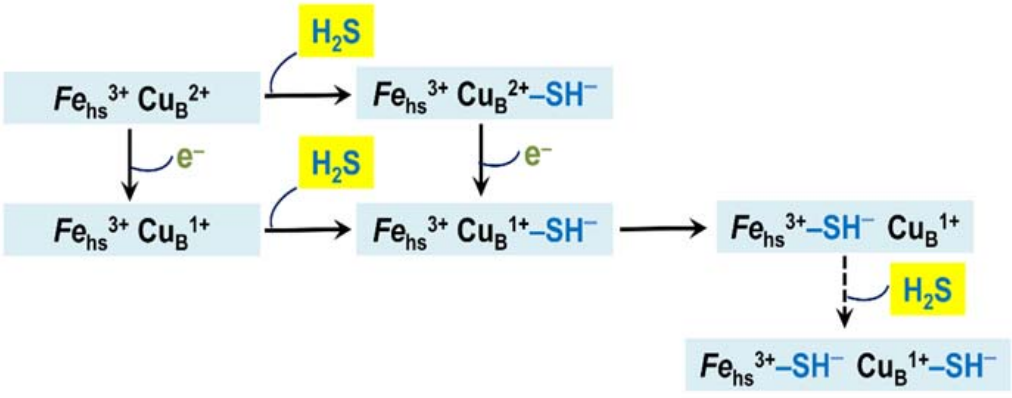

Figure 5. Proposed mechanism of inhibition of mitochondrial cytochrome *c* oxidase and *Escherichia coli* cytochrome bo_3 by H_2S. Shown is the catalytic binuclear center in different redox and ligation states. The center consists of the copper ion Cu_B and the high-spin heme (Fe_{hs}). The latter is heme a_3 in cytochrome *c* oxidase and heme o_3 in cytochrome bo_3. The metal redox groups which are not part of the center are not shown.

7. H_2S at Low Concentrations Serves as Electron Donor for Mitochondrial Cytochrome *c* Oxidase

H_2S at low concentrations can act as a substrate for mitochondrial complex IV (Figure 4) [36,37]. The fast form of the oxidized cytochrome *c* oxidase reacts aerobically with low H_2S levels in the absence of reduced substrates. However, the initial product of this reaction is not the inhibited enzyme but a catalytic intermediate, compound 'P' (Figure 6) [38]. Compound 'P' then decays into another catalytic intermediate, compound 'F'. It is proposed that in this reaction two H_2S molecules donate two electrons to the fully oxidized binuclear center, $a_3^{3+}Cu_B^{2+}$, converting it to the fully reduced state, $a_3^{2+}Cu_B^{+}$. The concomitant H_2S oxidation product is possibly hydrogen persulfide (HSSH), although a form of free sulfur (S^0 or S_8) cannot be excluded [38]. Then the fully reduced binuclear center reacts with O_2, producing compound 'P'. It remains unclear whether cytochrome *c* oxidase contributes significantly to a dissimilatory mechanism for the endogenously generated H_2S, or if SQOR is the major contributor in vivo. Notably, H_2S can also reduce complex IV indirectly, via reduction of its native substrate cytochrome *c* (Figure 4). The reaction between H_2S and cytochrome *c* presumably leads to the initial formation of the $HS^{\bullet}/S^{\bullet-}$ radical. $HS^{\bullet}/S^{\bullet-}$ could then be trapped by proteins producing protein persulfides and superoxide, or be trapped by O_2 yielding $HSO_2^{\bullet}$ [39].

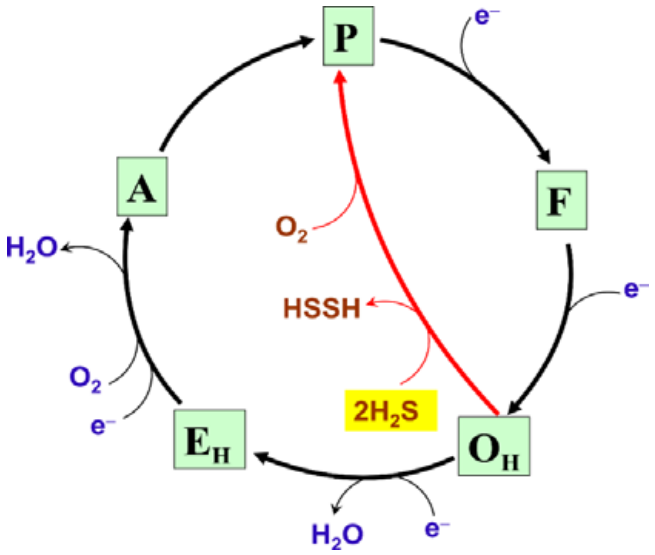

Figure 6. Proposed molecular mechanism of the reaction of the fast form of mitochondrial cytochrome *c* oxidase with low H_2S levels. O_H, E_H, A, P, and F are unrelaxed oxidized, unrelaxed one-electron-reduced, compound 'A', compound 'P', and compound 'F' catalytic intermediates, respectively. Chemical and pumped protons involved in the catalytic cycle are not shown for clarity.

8. Effect of H_2S on the Operation of the Branched Respiratory Chain of *E. coli* and Bacterial Growth

Under steady-state conditions, the mammalian tissue concentration of H_2S is usually in the low nanomolar range, e.g., it is around 15 nM in mouse brain and liver tissues [89]. The mammalian gut, in this sense, is unique among other body compartments. Millimolar concentrations (1.0–2.4 mM) of H_2S are commonly present in the gut [90]. The reason is that in the gastrointestinal tract, unlike other compartments, H_2S is generated by both the mammalian CBS, CSE, and 3MST, and by the microbial communities inhabiting the gut, of which sulfate-reducing bacteria are the key H_2S-producing species [90,91]. At such extremely high H_2S levels, bacterial respiratory chains which terminate in cytochrome *c* oxidase or other heme-copper oxidases should be inhibited. The question then arises as to how under these conditions bacteria inhabiting the mammalian gut can maintain aerobic respiration. It turned out that *E. coli*, and possibly other bacteria inhabiting H_2S-rich

environments, has a unique *bd*-type terminal oxidase that is not inhibited by H_2S, even at toxic concentrations [92–95].

E. coli is an essential member of the intestinal microbiome of humans and warm-blooded animals. The large intestine of humans normally harbors several *E. coli* strains at a given point in time [96]. In contrast to the electron transport chain of mammals that is unbranched, *E. coli*, like many other prokaryotes, possesses the branched aerobic respiratory chain (Figure 7) [45,97–102]. The *E. coli* chain comprises of type I and type II NADH dehydrogenases which transfer electrons from NADH to ubiquinol-8 (UQ8) or menaquinol-8 (MQ8); succinate dehydrogenase transferring electrons from succinate to UQ8; and three terminal oxidases, cytochromes bo_3, *bd*-I, and *bd*-II which transfer electrons from UQ8 or MQ8 to O_2 producing H_2O [103–112]. The proton motive force generated by type I NADH dehydrogenase and the terminal oxidases is used by F_oF_1-ATP synthase to make ATP [113–115]. Being a true proton pump, cytochrome bo_3 produces the proton motive force with higher efficiency as compared to the evolutionarily unrelated *bd*-type oxidases [116–121]. The three-dimensional structures of cytochrome bo_3 and cytochrome *bd*-I were determined [122–125]. The bo_3 oxidase is a member of type A-1 heme-copper oxidase superfamily [46,48,49,51,54,56–59,61–63]. Cytochrome bo_3 contains the UQ8 binding site, heme *b*, and the catalytic binuclear center formed by heme o_3 and Cu_B [101,126]. Cytochrome *bd*-I and cytochrome *bd*-II are members of the L subfamily of the cytochrome *bd* oxygen reductase family [127,128]. According to recent work by Murali et al. [129], the latter family should be expanded into a huge superfamily. The *bd* oxidase has the UQ8/MQ8 binding site, and three heme prosthetic groups, b_{558}, b_{595}, and *d* but lacks any copper site [97,98,108,127,130–133]. Hemes b_{595} and *d* may form a di-heme active site for oxygen chemistry, as evidenced by a number of studies [134–147]. These hemes are in van der Waals contacts [124,125], enabling fast electron transfers between them [119,145,146]. Thus, the functional di-heme active site in the *bd* oxidase implies that heme b_{595} is able to rapidly donate an electron and a proton to heme *d* to perform a concerted four-electron reduction of oxygen to water. This role of heme b_{595} in cytochrome *bd* is similar to that of Cu_B in the catalytic binuclear center of cytochrome bo_3. Cytochromes bo_3 and *bd* have low and high O_2 affinity, respectively [148–153]. As a consequence, the bo_3 enzyme dominates in *E. coli* under conditions of high O_2 concentration, whereas the *bd* oxidase is expressed at low aeration [154–158]. Cytochrome *bd* performs vital physiological functions in *E. coli* and other prokaryotes [16,131,159–163]. In particular, the enzyme endows the microbes with resistance to nitric oxide [164–173], peroxynitrite [160,174], hydrogen peroxide [16,175–180], cyanide [92,181,182], and ammonia [183]. The *bd*-type oxidases are present in the respiratory chains of bacteria and archaea but not in humans and animals. For this reason, they could serve as suitable protein targets for next-generation antibiotics [133,171,184–190].

Forte et al. studied the effect of H_2S on the oxygen consumption by the purified terminal oxidases bo_3, *bd*-I, and *bd*-II from *E. coli* [92]. It turned out that the activity of cytochrome bo_3 is quickly inhibited with an apparent half-maximal inhibitory concentration IC_{50} of 1.1 μM H_2S (pH 7.4). This value is similar to the K_i of 0.55 μM H_2S obtained by Nicholls and Kim for the beef heart cytochrome *c* oxidase at pH 7.48 [37]. The inhibition of the bo_3 oxidase appeared to be fully reversible. The rapid and total recovery of the enzymatic activity occurs following the removal of H_2S from the solution by the H_2S scavenger, the *Entamoeba histolytica O*-acetylserine sulfhydrylase (*Eh*OASS), in the presence of excess *O*-acetyl-L-serine (OAS). In contrast, neither the *bd*-I oxidase nor the *bd*-II oxidase is inhibited under identical conditions, even at a high concentration of H_2S (58 μM) [92]. Similar results were obtained when examining the effect of H_2S on the oxygen consumption by cell suspensions of the *E. coli* mutant strains which possess bo_3, *bd*-I, and *bd*-II as the only terminal oxidase. The oxygen uptake by cells having bo_3 as the sole oxidase is rapidly inhibited by 50 μM H_2S. As in the case of the purified enzyme, the inhibition is promptly and completely restored after H_2S depletion by the *Eh*OASS/OAS system. Conversely, H_2S at the same concentration does not affect the oxygen uptake by mutant cells having either

bd-I or *bd*-II as the only oxidase [92]. Similar data on the *E. coli* membrane vesicles were reported by Korshunov et al. [93].

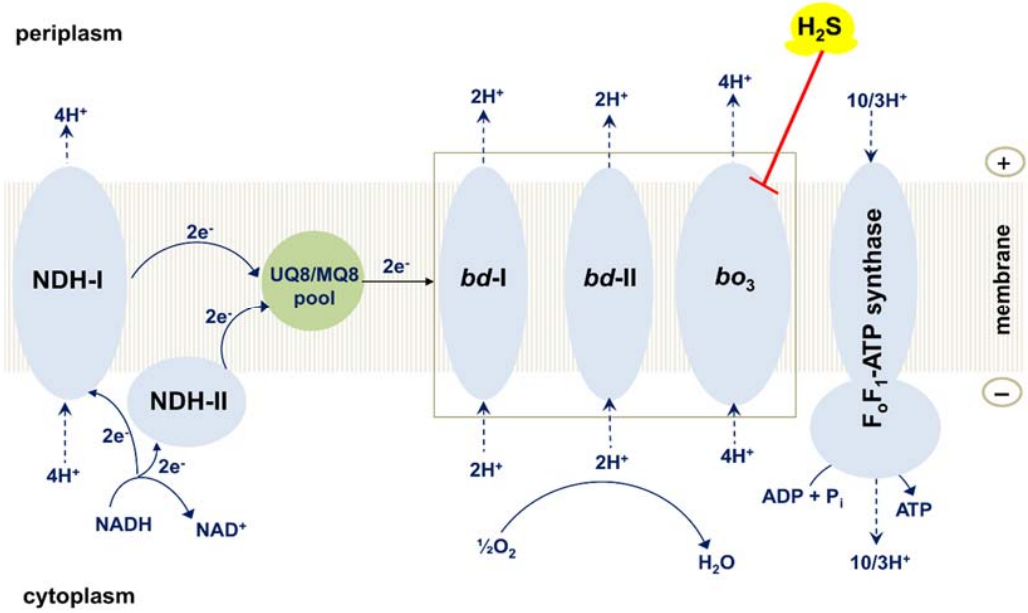

Figure 7. Effect of H_2S on the operation of the branched respiratory chain of *E. coli*. Shown is the schematic view of the branched aerobic respiratory chain of *E. coli*. H_2S inhibits cytochrome bo_3 but does not affect cytochrome *bd*-I and cytochrome *bd*-II. Succinate dehydrogenase and other substrate dehydrogenases are not shown for clarity.

Forte et al. also tested if *bd*-I and/or *bd*-II oxidases, besides enabling aerobic respiration, promote the growth of *E. coli* cells in the presence of H_2S [92]. A quantity of 200 μM H_2S appeared to severely inhibit the growth of mutant cells with only cytochrome bo_3. On the contrary, virtually no effect on cell growth was detected following the addition of H_2S at the same concentration to the strains which express either *bd*-I or *bd*-II as the sole oxidase. Thus, in contrast with cytochrome bo_3, which is potently and reversibly inhibited by H_2S, both cytochrome *bd*-I and cytochrome *bd*-II are H_2S-insensitive, and therefore, able to sustain respiration and cell growth in the presence of high levels of H_2S. We assume that the mechanism of the inhibition of the *E. coli* cytochrome bo_3 by H_2S is very similar to that suggested for the H_2S-mediated inhibition of another heme-copper terminal oxidase, mitochondrial complex IV (Figure 5).

The H_2S resistance of cytochrome *bd* is probably a key trait not only found in *E. coli*. Saini et al. [191] reported that H_2S promotes the respiration and growth of *Mycobacterium tuberculosis*, *Mycobacterium smegmatis*, and *Mycobacterium bovis* BCG. The authors concluded that the suppression of the cytochrome *bcc-aa*$_3$ supercomplex by H_2S leads to the switching of the electron flow from MQ to cytochrome *bd*. The latter, in turn, stimulates respiration and ATP production, leading to the increased growth of the mycobacteria [191]. Furthermore, Kunota et al. [192] showed that multidrug-resistant and drug-susceptible clinical *M. tuberculosis* strains (but not non-pathogenic *M. smegmatis*) generate H_2S endogenously, maintaining bioenergetic homeostasis by stimulating respiration primarily via the *bd*-type terminal oxidase. These findings are in agreement with the fact that the *bd* oxidases of the *E. coli* respiratory chain are H_2S-insensitive [92,93].

9. Concluding Remarks

Accumulated evidence has shown that H_2S is an effector molecule that controls energy metabolism. Depending on the concentration, H_2S can either stimulate or inhibit the mammalian mitochondrial respiratory chain and F_oF_1-ATP synthase. An involvement of LDHA in the stimulatory effects of H_2S on mitochondrial respiration has also been suggested. High H_2S inhibits the bacterial respiratory chain terminating in cytochrome bo_3

but not cytochrome *bd*. The effects of H_2S on a bacterial ATP synthase are still unknown. Although the role of H_2S in microorganisms has been investigated less, there is currently an explosion of interest in the link between H_2S and bacterial energy metabolism as a result of the recognition that this gaseous signaling molecule is critically important for the growth and colonization potential of pathogens, such as *M. tuberculosis*. A clearer picture of the effects of H_2S on energy metabolism would represent a significant advance for the development of novel therapeutics.

Author Contributions: V.B.B. and E.F. performed the literature review and wrote the paper. All authors have read and agreed to the published version of the manuscript.

Funding: This work was funded by the Russian Foundation for Basic Research (http://www.rfbr.ru/rffi/eng—research project № 19-04-00094) and Sapienza grants n. RP120172B8B36A98.

Institutional Review Board Statement: Not applicable.

Informed Consent Statement: Not applicable.

Acknowledgments: We are grateful to the anonymous reviewers for their comments and suggestions on this review.

Conflicts of Interest: The authors declare no conflict of interest. The funders had no role in the design of the study; in the collection, analyses, or interpretation of data; in the writing of the manuscript, or in the decision to publish the results.

References

1. Abe, K.; Kimura, H. The possible role of hydrogen sulfide as an endogenous neuromodulator. *J. Neurosci.* **1996**, *16*, 1066–1071. [CrossRef]
2. Yang, G.; Wu, L.; Jiang, B.; Yang, W.; Qi, J.; Cao, K.; Meng, Q.; Mustafa, A.K.; Mu, W.; Zhang, S.; et al. H_2S as a physiologic vasorelaxant: Hypertension in mice with deletion of cystathionine gamma-lyase. *Science* **2008**, *322*, 587–590. [CrossRef] [PubMed]
3. Bakalarz, D.; Korbut, E.; Yuan, Z.; Yu, B.; Wojcik, D.; Danielak, A.; Magierowska, K.; Kwiecien, S.; Brzozowski, T.; Marcinkowska, M.; et al. Novel hydrogen sulfide (H_2S)-releasing BW-HS-101 and its non-H_2S releasing derivative in modulation of microscopic and molecular parameters of gastric mucosal barrier. *Int. J. Mol. Sci.* **2021**, *22*, 5211. [CrossRef] [PubMed]
4. Nowaczyk, A.; Kowalska, M.; Nowaczyk, J.; Grzesk, G. Carbon monoxide and nitric oxide as examples of the youngest class of transmitters. *Int. J. Mol. Sci.* **2021**, *22*, 6029. [CrossRef]
5. Kimura, H. Production and physiological effects of hydrogen sulfide. *Antioxid. Redox Signal.* **2014**, *20*, 783–793. [CrossRef] [PubMed]
6. Wareham, L.K.; Southam, H.M.; Poole, R.K. Do nitric oxide, carbon monoxide and hydrogen sulfide really qualify as 'gasotransmitters' in bacteria? *Biochem. Soc. Trans.* **2018**, *46*, 1107–1118. [CrossRef]
7. Randi, E.B.; Zuhra, K.; Pecze, L.; Panagaki, T.; Szabo, C. Physiological concentrations of cyanide stimulate mitochondrial Complex IV and enhance cellular bioenergetics. *Proc. Natl. Acad. Sci. USA* **2021**, *118*, e2026245118. [CrossRef]
8. Giamogante, F.; Cali, T.; Malatesta, F. Physiological cyanide concentrations do not stimulate mitochondrial cytochrome *c* oxidase activity. *Proc. Natl. Acad. Sci. USA* **2021**, *118*, e2112373118. [CrossRef]
9. Zhao, W.; Zhang, J.; Lu, Y.; Wang, R. The vasorelaxant effect of H_2S as a novel endogenous gaseous K_{ATP} channel opener. *Embo J.* **2001**, *20*, 6008–6016. [CrossRef]
10. Papapetropoulos, A.; Pyriochou, A.; Altaany, Z.; Yang, G.; Marazioti, A.; Zhou, Z.; Jeschke, M.G.; Branski, L.K.; Herndon, D.N.; Wang, R.; et al. Hydrogen sulfide is an endogenous stimulator of angiogenesis. *Proc. Natl. Acad. Sci. USA* **2009**, *106*, 21972–21977. [CrossRef]
11. Yang, G.; Sun, X.; Wang, R. Hydrogen sulfide-induced apoptosis of human aorta smooth muscle cells via the activation of mitogen-activated protein kinases and caspase-3. *FASEB J.* **2004**, *18*, 1782–1784. [CrossRef] [PubMed]
12. Murphy, B.; Bhattacharya, R.; Mukherjee, P. Hydrogen sulfide signaling in mitochondria and disease. *FASEB J.* **2019**, *33*, 13098–13125. [CrossRef] [PubMed]
13. Cao, X.; Ding, L.; Xie, Z.Z.; Yang, Y.; Whiteman, M.; Moore, P.K.; Bian, J.S. A review of hydrogen sulfide synthesis, metabolism, and measurement: Is modulation of hydrogen sulfide a novel therapeutic for cancer? *Antioxid. Redox Signal.* **2019**, *31*, 1–38. [CrossRef] [PubMed]
14. Corpas, F.J.; Palma, J.M. H_2S signaling in plants and applications in agriculture. *J. Adv. Res.* **2020**, *24*, 131–137. [CrossRef]
15. Shatalin, K.; Shatalina, E.; Mironov, A.; Nudler, E. H_2S: A universal defense against antibiotics in bacteria. *Science* **2011**, *334*, 986–990. [CrossRef]
16. Borisov, V.B.; Siletsky, S.A.; Nastasi, M.R.; Forte, E. ROS defense systems and terminal oxidases in bacteria. *Antioxidants* **2021**, *10*, 839. [CrossRef]

17. Calhoun, D.B.; Englander, S.W.; Wright, W.W.; Vanderkooi, J.M. Quenching of room temperature protein phosphorescence by added small molecules. *Biochemistry* **1988**, *27*, 8466–8474. [CrossRef]
18. Riahi, S.; Rowley, C.N. Why can hydrogen sulfide permeate cell membranes? *J. Am. Chem. Soc.* **2014**, *136*, 15111–15113. [CrossRef]
19. Li, Q.; Lancaster, J.R., Jr. Chemical foundations of hydrogen sulfide biology. *Nitric Oxide* **2013**, *35*, 21–34. [CrossRef]
20. Llopis, J.; McCaffery, J.M.; Miyawaki, A.; Farquhar, M.G.; Tsien, R.Y. Measurement of cytosolic, mitochondrial, and Golgi pH in single living cells with green fluorescent proteins. *Proc. Natl. Acad. Sci. USA* **1998**, *95*, 6803–6808. [CrossRef]
21. Abad, M.F.; Di Benedetto, G.; Magalhaes, P.J.; Filippin, L.; Pozzan, T. Mitochondrial pH monitored by a new engineered green fluorescent protein mutant. *J. Biol. Chem.* **2004**, *279*, 11521–11529. [CrossRef] [PubMed]
22. Ohkuma, S.; Poole, B. Fluorescence probe measurement of the intralysosomal pH in living cells and the perturbation of pH by various agents. *Proc. Natl. Acad. Sci. USA* **1978**, *75*, 3327–3331. [CrossRef]
23. Powell, C.R.; Dillon, K.M.; Matson, J.B. A review of hydrogen sulfide (H_2S) donors: Chemistry and potential therapeutic applications. *Biochem. Pharmacol.* **2018**, *149*, 110–123. [CrossRef]
24. Yang, J.; Minkler, P.; Grove, D.; Wang, R.; Willard, B.; Dweik, R.; Hine, C. Non-enzymatic hydrogen sulfide production from cysteine in blood is catalyzed by iron and vitamin B_6. *Commun. Biol.* **2019**, *2*, 194. [CrossRef]
25. Kabil, O.; Vitvitsky, V.; Xie, P.; Banerjee, R. The quantitative significance of the transsulfuration enzymes for H_2S production in murine tissues. *Antioxid. Redox Signal.* **2011**, *15*, 363–372. [CrossRef] [PubMed]
26. Giuffre, A.; Vicente, J.B. Hydrogen sulfide biochemistry and interplay with other gaseous mediators in mammalian physiology. *Oxid. Med. Cell. Longev.* **2018**, *2018*, 6290931. [CrossRef] [PubMed]
27. Shatalin, K.; Nuthanakanti, A.; Kaushik, A.; Shishov, D.; Peselis, A.; Shamovsky, I.; Pani, B.; Lechpammer, M.; Vasilyev, N.; Shatalina, E.; et al. Inhibitors of bacterial H_2S biogenesis targeting antibiotic resistance and tolerance. *Science* **2021**, *372*, 1169–1175. [CrossRef]
28. Caruana, N.J.; Stroud, D.A. The road to the structure of the mitochondrial respiratory chain supercomplex. *Biochem. Soc. Trans.* **2020**, *48*, 621–629. [CrossRef]
29. Cogliati, S.; Cabrera-Alarcon, J.L.; Enriquez, J.A. Regulation and functional role of the electron transport chain supercomplexes. *Biochem. Soc. Trans.* **2021**, BST20210460. [CrossRef]
30. Modis, K.; Ju, Y.; Ahmad, A.; Untereiner, A.A.; Altaany, Z.; Wu, L.; Szabo, C.; Wang, R. *S*-Sulfhydration of ATP synthase by hydrogen sulfide stimulates mitochondrial bioenergetics. *Pharmacol. Res.* **2016**, *113*, 116–124. [CrossRef]
31. Untereiner, A.A.; Olah, G.; Modis, K.; Hellmich, M.R.; Szabo, C. H_2S-induced S-sulfhydration of lactate dehydrogenase a (LDHA) stimulates cellular bioenergetics in HCT116 colon cancer cells. *Biochem. Pharmacol.* **2017**, *136*, 86–98. [CrossRef] [PubMed]
32. Goubern, M.; Andriamihaja, M.; Nubel, T.; Blachier, F.; Bouillaud, F. Sulfide, the first inorganic substrate for human cells. *FASEB J.* **2007**, *21*, 1699–1706. [CrossRef] [PubMed]
33. Nicholls, P. The effect of sulphide on cytochrome aa_3. Isosteric and allosteric shifts of the reduced α-peak. *Biochim. Biophys. Acta* **1975**, *396*, 24–35. [CrossRef]
34. Petersen, L.C. The effect of inhibitors on the oxygen kinetics of cytochrome *c* oxidase. *Biochim. Biophys. Acta* **1977**, *460*, 299–307. [CrossRef]
35. Szabo, C.; Ransy, C.; Modis, K.; Andriamihaja, M.; Murghes, B.; Coletta, C.; Olah, G.; Yanagi, K.; Bouillaud, F. Regulation of mitochondrial bioenergetic function by hydrogen sulfide. Part I. Biochemical and physiological mechanisms. *Br. J. Pharmacol.* **2014**, *171*, 2099–2122. [CrossRef] [PubMed]
36. Nicholls, P.; Kim, J.K. Oxidation of sulphide by cytochrome aa_3. *Biochim. Biophys. Acta* **1981**, *637*, 312–320. [CrossRef]
37. Nicholls, P.; Kim, J.K. Sulphide as an inhibitor and electron donor for the cytochrome *c* oxidase system. *Can. J. Biochem.* **1982**, *60*, 613–623. [CrossRef] [PubMed]
38. Nicholls, P.; Marshall, D.C.; Cooper, C.E.; Wilson, M.T. Sulfide inhibition of and metabolism by cytochrome *c* oxidase. *Biochem. Soc. Trans.* **2013**, *41*, 1312–1316. [CrossRef]
39. Vitvitsky, V.; Miljkovic, J.L.; Bostelaar, T.; Adhikari, B.; Yadav, P.K.; Steiger, A.K.; Torregrossa, R.; Pluth, M.D.; Whiteman, M.; Banerjee, R.; et al. Cytochrome *c* reduction by H_2S potentiates sulfide signaling. *ACS Chem. Biol.* **2018**, *13*, 2300–2307. [CrossRef]
40. Doherty, J.R.; Cleveland, J.L. Targeting lactate metabolism for cancer therapeutics. *J. Clin. Invest.* **2013**, *123*, 3685–3692. [CrossRef]
41. Powell, M.A.; Somero, G.N. Hydrogen sulfide oxidation Is coupled to oxidative phosphorylation in mitochondria of *Solemya reidi*. *Science* **1986**, *233*, 563–566. [CrossRef]
42. Landry, A.P.; Ballou, D.P.; Banerjee, R. Hydrogen sulfide oxidation by sulfide quinone oxidoreductase. *Chembiochem* **2021**, *22*, 949–960. [CrossRef] [PubMed]
43. Landry, A.P.; Moon, S.; Kim, H.; Yadav, P.K.; Guha, A.; Cho, U.S.; Banerjee, R. A catalytic trisulfide in human sulfide quinone oxidoreductase catalyzes Coenzyme A persulfide synthesis and inhibits butyrate oxidation. *Cell Chem. Biol.* **2019**, *26*, 1515–1525.e1514. [CrossRef] [PubMed]
44. Malatesta, F.; Antonini, G.; Sarti, P.; Brunori, M. Structure and function of a molecular machine: Cytochrome *c* oxidase. *Biophys. Chem.* **1995**, *54*, 1–33. [CrossRef]
45. Melo, A.M.; Teixeira, M. Supramolecular organization of bacterial aerobic respiratory chains: From cells and back. *Biochim. Biophys. Acta* **2016**, *1857*, 190–197. [CrossRef]
46. Siletsky, S.A.; Borisov, V.B.; Mamedov, M.D. Photosystem II and terminal respiratory oxidases: Molecular machines operating in opposite directions. *Front. Biosci.* **2017**, *22*, 1379–1426. [CrossRef]

47. Pereira, M.M.; Sousa, F.L.; Verissimo, A.F.; Teixeira, M. Looking for the minimum common denominator in haem-copper oxygen reductases: Towards a unified catalytic mechanism. *Biochim. Biophys. Acta* **2008**, *1777*, 929–934. [CrossRef]
48. Pereira, M.M.; Santana, M.; Teixeira, M. A novel scenario for the evolution of haem-copper oxygen reductases. *Biochim. Biophys. Acta* **2001**, *1505*, 185–208. [CrossRef]
49. Pereira, M.M.; Gomes, C.M.; Teixeira, M. Plasticity of proton pathways in haem-copper oxygen reductases. *FEBS Lett.* **2002**, *522*, 14–18. [CrossRef]
50. Pereira, M.M.; Teixeira, M. Proton pathways, ligand binding and dynamics of the catalytic site in haem-copper oxygen reductases: A comparison between the three families. *Biochim. Biophys. Acta* **2004**, *1655*, 340–346. [CrossRef]
51. Papa, S.; Capitanio, N.; Capitanio, G.; Palese, L.L. Protonmotive cooperativity in cytochrome *c* oxidase. *Biochim. Biophys. Acta* **2004**, *1658*, 95–105. [CrossRef]
52. Borisov, V.B. Defects in mitochondrial respiratory complexes III and IV, and human pathologies. *Mol. Aspects Med.* **2002**, *23*, 385–412. [CrossRef]
53. Borisov, V.B. Mutations in respiratory chain complexes and human diseases. *Ital. J. Biochem.* **2004**, *53*, 34–40.
54. Borisov, V.B.; Siletsky, S.A. Features of organization and mechanism of catalysis of two families of terminal oxidases: Heme-copper and *bd*-type. *Biochemistry* **2019**, *84*, 1390–1402. [CrossRef] [PubMed]
55. Hederstedt, L. Molecular biology of *Bacillus subtilis* cytochromes *anno* 2020. *Biochemistry* **2021**, *86*, 8–21. [CrossRef]
56. Sousa, F.L.; Alves, R.J.; Ribeiro, M.A.; Pereira-Leal, J.B.; Teixeira, M.; Pereira, M.M. The superfamily of heme-copper oxygen reductases: Types and evolutionary considerations. *Biochim. Biophys. Acta* **2012**, *1817*, 629–637. [CrossRef] [PubMed]
57. Wikstrom, M.; Krab, K.; Sharma, V. Oxygen activation and energy conservation by cytochrome *c* oxidase. *Chem. Rev.* **2018**, *118*, 2469–2490. [CrossRef] [PubMed]
58. Capitanio, N.; Palese, L.L.; Capitanio, G.; Martino, P.L.; Richter, O.M.; Ludwig, B.; Papa, S. Allosteric interactions and proton conducting pathways in proton pumping aa_3 oxidases: Heme *a* as a key coupling element. *Biochim. Biophys. Acta* **2012**, *1817*, 558–566. [CrossRef] [PubMed]
59. Maneg, O.; Malatesta, F.; Ludwig, B.; Drosou, V. Interaction of cytochrome *c* with cytochrome oxidase: Two different docking scenarios. *Biochim. Biophys. Acta* **2004**, *1655*, 274–281. [CrossRef]
60. Gavrikova, E.V.; Grivennikova, V.G.; Borisov, V.B.; Cecchini, G.; Vinogradov, A.D. Assembly of a chimeric respiratory chain from bovine heart submitochondrial particles and cytochrome *bd* terminal oxidase of *Escherichia coli*. *FEBS Lett.* **2009**, *583*, 1287–1291. [CrossRef]
61. von Ballmoos, C.; Adelroth, P.; Gennis, R.B.; Brzezinski, P. Proton transfer in ba_3 cytochrome *c* oxidase from *Thermus thermophilus*. *Biochim. Biophys. Acta* **2012**, *1817*, 650–657. [CrossRef] [PubMed]
62. Rich, P.R. Mitochondrial cytochrome *c* oxidase: Catalysis, coupling and controversies. *Biochem. Soc. Trans.* **2017**, *45*, 813–829. [CrossRef]
63. Yoshikawa, S.; Shimada, A. Reaction mechanism of cytochrome *c* oxidase. *Chem. Rev.* **2015**, *115*, 1936–1989. [CrossRef]
64. Forte, E.; Giuffre, A.; Huang, L.S.; Berry, E.A.; Borisov, V.B. Nitric oxide does not inhibit but is metabolized by the cytochrome *bcc-aa*$_3$ supercomplex. *Int. J. Mol. Sci.* **2020**, *21*, 8521. [CrossRef] [PubMed]
65. Siletsky, S.A.; Borisov, V.B. Proton pumping and non-pumping terminal respiratory oxidases: Active sites intermediates of these molecular machines and their derivatives. *Int. J. Mol. Sci.* **2021**, *22*, 10852. [CrossRef]
66. Tsukihara, T.; Aoyama, H.; Yamashita, E.; Tomizaki, T.; Yamaguchi, H.; Shinzawa-Itoh, K.; Nakashima, R.; Yaono, R.; Yoshikawa, S. The whole structure of the 13-subunit oxidized cytochrome *c* oxidase at 2.8 A. *Science* **1996**, *272*, 1136–1144. [CrossRef] [PubMed]
67. Yano, N.; Muramoto, K.; Shimada, A.; Takemura, S.; Baba, J.; Fujisawa, H.; Mochizuki, M.; Shinzawa-Itoh, K.; Yamashita, E.; Tsukihara, T.; et al. The Mg^{2+}-containing water cluster of mammalian cytochrome *c* oxidase collects four pumping proton equivalents in each catalytic cycle. *J. Biol. Chem.* **2016**, *291*, 23882–23894. [CrossRef]
68. Shimada, A.; Etoh, Y.; Kitoh-Fujisawa, R.; Sasaki, A.; Shinzawa-Itoh, K.; Hiromoto, T.; Yamashita, E.; Muramoto, K.; Tsukihara, T.; Yoshikawa, S. X-ray structures of catalytic intermediates of cytochrome *c* oxidase provide insights into its O_2 activation and unidirectional proton-pump mechanisms. *J. Biol. Chem.* **2020**, *295*, 5818–5833. [CrossRef]
69. Shimada, A.; Hara, F.; Shinzawa-Itoh, K.; Kanehisa, N.; Yamashita, E.; Muramoto, K.; Tsukihara, T.; Yoshikawa, S. Critical roles of the Cu_B site in efficient proton pumping as revealed by crystal structures of mammalian cytochrome *c* oxidase catalytic intermediates. *J. Biol. Chem.* **2021**, *297*, 100967. [CrossRef]
70. Antonini, E.; Brunori, M.; Colosimo, A.; Greenwood, C.; Wilson, M.T. Oxygen "pulsed" cytochrome c oxidase: Functional properties and catalytic relevance. *Proc. Natl. Acad. Sci. USA* **1977**, *74*, 3128–3132. [CrossRef]
71. Moody, A.J. "As prepared" forms of fully oxidised haem/Cu terminal oxidases. *Biochim. Biophys. Acta* **1996**, *1276*, 6–20. [CrossRef]
72. Moody, A.J.; Cooper, C.E.; Rich, P.R. Characterisation of 'fast' and 'slow' forms of bovine heart cytochrome-*c* oxidase. *Biochim. Biophys. Acta* **1991**, *1059*, 189–207. [CrossRef]
73. Cooper, C.E.; Brown, G.C. The inhibition of mitochondrial cytochrome oxidase by the gases carbon monoxide, nitric oxide, hydrogen cyanide and hydrogen sulfide: Chemical mechanism and physiological significance. *J. Bioenerg. Biomembr.* **2008**, *40*, 533–539. [CrossRef] [PubMed]
74. Khan, A.A.; Schuler, M.M.; Prior, M.G.; Yong, S.; Coppock, R.W.; Florence, L.Z.; Lillie, L.E. Effects of hydrogen sulfide exposure on lung mitochondrial respiratory chain enzymes in rats. *Toxicol. Appl. Pharmacol.* **1990**, *103*, 482–490. [CrossRef]

75. Khan, A.A.; Yong, S.; Prior, M.G.; Lillie, L.E. Cytotoxic effects of hydrogen sulfide on pulmonary alveolar macrophages in rats. *J. Toxicol. Environ. Health* **1991**, *33*, 57–64. [CrossRef]
76. Struve, M.F.; Brisbois, J.N.; James, R.A.; Marshall, M.W.; Dorman, D.C. Neurotoxicological effects associated with short-term exposure of Sprague-Dawley rats to hydrogen sulfide. *Neurotoxicology* **2001**, *22*, 375–385. [CrossRef]
77. Dorman, D.C.; Moulin, F.J.; McManus, B.E.; Mahle, K.C.; James, R.A.; Struve, M.F. Cytochrome oxidase inhibition induced by acute hydrogen sulfide inhalation: Correlation with tissue sulfide concentrations in the rat brain, liver, lung, and nasal epithelium. *Toxicol. Sci.* **2002**, *65*, 18–25. [CrossRef]
78. Dorman, D.C.; Struve, M.F.; Gross, E.A.; Brenneman, K.A. Respiratory tract toxicity of inhaled hydrogen sulfide in Fischer-344 rats, Sprague-Dawley rats, and B6C3F1 mice following subchronic (90-day) exposure. *Toxicol. Appl. Pharmacol.* **2004**, *198*, 29–39. [CrossRef]
79. Wu, N.; Du, X.; Wang, D.; Hao, F. Myocardial and lung injuries induced by hydrogen sulfide and the effectiveness of oxygen therapy in rats. *Clin. Toxicol.* **2011**, *49*, 161–166. [CrossRef]
80. Thompson, R.W.; Valentine, H.L.; Valentine, W.M. Cytotoxic mechanisms of hydrosulfide anion and cyanide anion in primary rat hepatocyte cultures. *Toxicology* **2003**, *188*, 149–159. [CrossRef]
81. Leschelle, X.; Goubern, M.; Andriamihaja, M.; Blottiere, H.M.; Couplan, E.; Gonzalez-Barroso, M.D.; Petit, C.; Pagniez, A.; Chaumontet, C.; Mignotte, B.; et al. Adaptative metabolic response of human colonic epithelial cells to the adverse effects of the luminal compound sulfide. *Biochim. Biophys. Acta* **2005**, *1725*, 201–212. [CrossRef]
82. Truong, D.H.; Eghbal, M.A.; Hindmarsh, W.; Roth, S.H.; O'Brien, P.J. Molecular mechanisms of hydrogen sulfide toxicity. *Drug Metab. Rev.* **2006**, *38*, 733–744. [CrossRef]
83. Sun, W.H.; Liu, F.; Chen, Y.; Zhu, Y.C. Hydrogen sulfide decreases the levels of ROS by inhibiting mitochondrial complex IV and increasing SOD activities in cardiomyocytes under ischemia/reperfusion. *Biochem. Biophys. Res. Commun.* **2012**, *421*, 164–169. [CrossRef] [PubMed]
84. Groeger, M.; Matallo, J.; McCook, O.; Wagner, F.; Wachter, U.; Bastian, O.; Gierer, S.; Reich, V.; Stahl, B.; Huber-Lang, M.; et al. Temperature and cell-type dependency of sulfide effects on mitochondrial respiration. *Shock* **2012**, *38*, 367–374. [CrossRef] [PubMed]
85. Buckler, K.J. Effects of exogenous hydrogen sulphide on calcium signalling, background (TASK) K channel activity and mitochondrial function in chemoreceptor cells. *Pflugers Arch.* **2012**, *463*, 743–754. [CrossRef] [PubMed]
86. Di Meo, I.; Fagiolari, G.; Prelle, A.; Viscomi, C.; Zeviani, M.; Tiranti, V. Chronic exposure to sulfide causes accelerated degradation of cytochrome *c* oxidase in ethylmalonic encephalopathy. *Antioxid. Redox Signal.* **2011**, *15*, 353–362. [CrossRef] [PubMed]
87. Nicholls, P.; Petersen, L.C.; Miller, M.; Hansen, F.B. Ligand-induced spectral changes in cytochrome *c* oxidase and their possible significance. *Biochim. Biophys. Acta* **1976**, *449*, 188–196. [CrossRef]
88. Hill, B.C.; Woon, T.C.; Nicholls, P.; Peterson, J.; Greenwood, C.; Thomson, A.J. Interactions of sulphide and other ligands with cytochrome *c* oxidase. An electron-paramagnetic-resonance study. *Biochem. J.* **1984**, *224*, 591–600. [CrossRef]
89. Furne, J.; Saeed, A.; Levitt, M.D. Whole tissue hydrogen sulfide concentrations are orders of magnitude lower than presently accepted values. *Am. J. Physiol. Regul. Integr. Comp. Physiol.* **2008**, *295*, R1479–R1485. [CrossRef]
90. Dordevic, D.; Jancikova, S.; Vitezova, M.; Kushkevych, I. Hydrogen sulfide toxicity in the gut environment: Meta-analysis of sulfate-reducing and lactic acid bacteria in inflammatory processes. *J. Adv. Res.* **2020**, *27*, 55–69. [CrossRef]
91. Carbonero, F.; Benefiel, A.C.; Alizadeh-Ghamsari, A.H.; Gaskins, H.R. Microbial pathways in colonic sulfur metabolism and links with health and disease. *Front. Physiol.* **2012**, *3*, 448. [CrossRef]
92. Forte, E.; Borisov, V.B.; Falabella, M.; Colaco, H.G.; Tinajero-Trejo, M.; Poole, R.K.; Vicente, J.B.; Sarti, P.; Giuffre, A. The terminal oxidase cytochrome *bd* promotes sulfide-resistant bacterial respiration and growth. *Sci. Rep.* **2016**, *6*, 23788. [CrossRef] [PubMed]
93. Korshunov, S.; Imlay, K.R.; Imlay, J.A. The cytochrome *bd* oxidase of *Escherichia coli* prevents respiratory inhibition by endogenous and exogenous hydrogen sulfide. *Mol. Microbiol.* **2016**, *101*, 62–77. [CrossRef]
94. Forte, E.; Giuffre, A. How bacteria breathe in hydrogen sulphide-rich environments. *Biochemist* **2016**, *38*, 8–11. [CrossRef]
95. Borisov, V.B.; Forte, E. Terminal oxidase cytochrome *bd* protects bacteria against hydrogen sulfide toxicity. *Biochemistry* **2021**, *86*, 22–32. [CrossRef] [PubMed]
96. Karami, N.; Nowrouzian, F.; Adlerberth, I.; Wold, A.E. Tetracycline resistance in *Escherichia coli* and persistence in the infantile colonic microbiota. *Antimicrob. Agents Chemother.* **2006**, *50*, 156–161. [CrossRef]
97. Poole, R.K.; Cook, G.M. Redundancy of aerobic respiratory chains in bacteria? Routes, reasons and regulation. *Adv. Microb. Physiol.* **2000**, *43*, 165–224. [CrossRef]
98. Ingledew, W.J.; Poole, R.K. The respiratory chains of *Escherichia coli*. *Microbiol. Rev.* **1984**, *48*, 222–271. [CrossRef]
99. Azarkina, N.; Borisov, V.; Konstantinov, A.A. Spontaneous spectral changes of the reduced cytochrome *bd*. *FEBS Lett.* **1997**, *416*, 171–174. [CrossRef]
100. Erhardt, H.; Dempwolff, F.; Pfreundschuh, M.; Riehle, M.; Schafer, C.; Pohl, T.; Graumann, P.; Friedrich, T. Organization of the *Escherichia coli* aerobic enzyme complexes of oxidative phosphorylation in dynamic domains within the cytoplasmic membrane. *Microbiologyopen* **2014**, *3*, 316–326. [CrossRef]
101. Borisov, V.B.; Verkhovsky, M.I. Oxygen as Acceptor. *EcoSal Plus* **2015**, *6*. [CrossRef] [PubMed]
102. Azarkina, N.; Siletsky, S.; Borisov, V.; von Wachenfeldt, C.; Hederstedt, L.; Konstantinov, A.A. A cytochrome bb'-type quinol oxidase in *Bacillus subtilis* strain 168. *J. Biol. Chem.* **1999**, *274*, 32810–32817. [CrossRef] [PubMed]

103. Melin, F.; Sabuncu, S.; Choi, S.K.; Leprince, A.; Gennis, R.B.; Hellwig, P. Role of the tightly bound quinone for the oxygen reaction of cytochrome bo_3 oxidase from *Escherichia coli*. *FEBS Lett.* **2018**, *592*, 3380–3387. [CrossRef] [PubMed]
104. Szundi, I.; Kittredge, C.; Choi, S.K.; McDonald, W.; Ray, J.; Gennis, R.B.; Einarsdottir, O. Kinetics and intermediates of the reaction of fully reduced *Escherichia coli* bo_3 ubiquinol oxidase with O_2. *Biochemistry* **2014**, *53*, 5393–5404. [CrossRef]
105. Mogi, T.; Tsubaki, M.; Hori, H.; Miyoshi, H.; Nakamura, H.; Anraku, Y. Two terminal quinol oxidase families in *Escherichia coli*: Variations on molecular machinery for dioxygen reduction. *J. Biochem. Mol. Biol. Biophys.* **1998**, *2*, 79–110.
106. Svensson Ek, M.; Brzezinski, P. Oxidation of ubiquinol by cytochrome bo_3 from *Escherichia coli*: Kinetics of electron and proton transfer. *Biochemistry* **1997**, *36*, 5425–5431. [CrossRef]
107. Yang, K.; Borisov, V.B.; Konstantinov, A.A.; Gennis, R.B. The fully oxidized form of the cytochrome *bd* quinol oxidase from *E. coli* does not participate in the catalytic cycle: Direct evidence from rapid kinetics studies. *FEBS Lett.* **2008**, *582*, 3705–3709. [CrossRef]
108. Junemann, S. Cytochrome *bd* terminal oxidase. *Biochim. Biophys. Acta* **1997**, *1321*, 107–127. [CrossRef]
109. Borisov, V.B.; Forte, E.; Sarti, P.; Giuffre, A. Catalytic intermediates of cytochrome *bd* terminal oxidase at steady-state: Ferryl and oxy-ferrous species dominate. *Biochim. Biophys. Acta* **2011**, *1807*, 503–509. [CrossRef]
110. Li, M.; Jorgensen, S.K.; McMillan, D.G.; Krzeminski, L.; Daskalakis, N.N.; Partanen, R.H.; Tutkus, M.; Tuma, R.; Stamou, D.; Hatzakis, N.S.; et al. Single enzyme experiments reveal a long-lifetime proton leak state in a heme-copper oxidase. *J. Am. Chem. Soc.* **2015**, *137*, 16055–16063. [CrossRef]
111. Asseri, A.H.; Godoy-Hernandez, A.; Goojani, H.G.; Lill, H.; Sakamoto, J.; McMillan, D.G.G.; Bald, D. Cardiolipin enhances the enzymatic activity of cytochrome *bd* and cytochrome bo_3 solubilized in dodecyl-maltoside. *Sci. Rep.* **2021**, *11*, 8006. [CrossRef] [PubMed]
112. Nikolaev, A.; Safarian, S.; Thesseling, A.; Wohlwend, D.; Friedrich, T.; Michel, H.; Kusumoto, T.; Sakamoto, J.; Melin, F.; Hellwig, P. Electrocatalytic evidence of the diversity of the oxygen reaction in the bacterial *bd* oxidase from different organisms. *Biochim. Biophys. Acta Bioenerg.* **2021**, *1862*, 148436. [CrossRef] [PubMed]
113. Nakanishi-Matsui, M.; Sekiya, M.; Futai, M. ATP synthase from *Escherichia coli*: Mechanism of rotational catalysis, and inhibition with the epsilon subunit and phytopolyphenols. *Biochim. Biophys. Acta* **2016**, *1857*, 129–140. [CrossRef] [PubMed]
114. Deckers-Hebestreit, G.; Greie, J.; Stalz, W.; Altendorf, K. The ATP synthase of *Escherichia coli*: Structure and function of F_0 subunits. *Biochim. Biophys. Acta* **2000**, *1458*, 364–373. [CrossRef]
115. Sobti, M.; Walshe, J.L.; Wu, D.; Ishmukhametov, R.; Zeng, Y.C.; Robinson, C.V.; Berry, R.M.; Stewart, A.G. Cryo-EM structures provide insight into how *E. coli* F_1F_o ATP synthase accommodates symmetry mismatch. *Nat. Commun.* **2020**, *11*, 2615. [CrossRef]
116. Puustinen, A.; Finel, M.; Haltia, T.; Gennis, R.B.; Wikstrom, M. Properties of the two terminal oxidases of *Escherichia coli*. *Biochemistry* **1991**, *30*, 3936–3942. [CrossRef]
117. Jasaitis, A.; Borisov, V.B.; Belevich, N.P.; Morgan, J.E.; Konstantinov, A.A.; Verkhovsky, M.I. Electrogenic reactions of cytochrome *bd*. *Biochemistry* **2000**, *39*, 13800–13809. [CrossRef]
118. Belevich, I.; Borisov, V.B.; Zhang, J.; Yang, K.; Konstantinov, A.A.; Gennis, R.B.; Verkhovsky, M.I. Time-resolved electrometric and optical studies on cytochrome *bd* suggest a mechanism of electron-proton coupling in the di-heme active site. *Proc. Natl. Acad. Sci. USA* **2005**, *102*, 3657–3662. [CrossRef]
119. Belevich, I.; Borisov, V.B.; Verkhovsky, M.I. Discovery of the true peroxy intermediate in the catalytic cycle of terminal oxidases by real-time measurement. *J. Biol. Chem.* **2007**, *282*, 28514–28519. [CrossRef]
120. Borisov, V.B.; Belevich, I.; Bloch, D.A.; Mogi, T.; Verkhovsky, M.I. Glutamate 107 in subunit I of cytochrome *bd* from *Escherichia coli* is part of a transmembrane intraprotein pathway conducting protons from the cytoplasm to the heme b_{595}/heme *d* active site. *Biochemistry* **2008**, *47*, 7907–7914. [CrossRef]
121. Borisov, V.B.; Murali, R.; Verkhovskaya, M.L.; Bloch, D.A.; Han, H.; Gennis, R.B.; Verkhovsky, M.I. Aerobic respiratory chain of *Escherichia coli* is not allowed to work in fully uncoupled mode. *Proc. Natl. Acad. Sci. USA* **2011**, *108*, 17320–17324. [CrossRef]
122. Abramson, J.; Riistama, S.; Larsson, G.; Jasaitis, A.; Svensson-Ek, M.; Laakkonen, L.; Puustinen, A.; Iwata, S.; Wikstrom, M. The structure of the ubiquinol oxidase from *Escherichia coli* and its ubiquinone binding site. *Nat. Struct. Biol.* **2000**, *7*, 910–917. [CrossRef] [PubMed]
123. Li, J.; Han, L.; Vallese, F.; Ding, Z.; Choi, S.K.; Hong, S.; Luo, Y.; Liu, B.; Chan, C.K.; Tajkhorshid, E.; et al. Cryo-EM structures of *Escherichia coli* cytochrome bo_3 reveal bound phospholipids and ubiquinone-8 in a dynamic substrate binding site. *Proc. Natl. Acad. Sci. USA* **2021**, *118*, e2106750118. [CrossRef] [PubMed]
124. Safarian, S.; Hahn, A.; Mills, D.J.; Radloff, M.; Eisinger, M.L.; Nikolaev, A.; Meier-Credo, J.; Melin, F.; Miyoshi, H.; Gennis, R.B.; et al. Active site rearrangement and structural divergence in prokaryotic respiratory oxidases. *Science* **2019**, *366*, 100–104. [CrossRef]
125. Thesseling, A.; Rasmussen, T.; Burschel, S.; Wohlwend, D.; Kagi, J.; Muller, R.; Bottcher, B.; Friedrich, T. Homologous *bd* oxidases share the same architecture but differ in mechanism. *Nat. Commun.* **2019**, *10*, 5138. [CrossRef]
126. Choi, S.K.; Schurig-Briccio, L.; Ding, Z.; Hong, S.; Sun, C.; Gennis, R.B. Location of the substrate binding site of the cytochrome bo_3 ubiquinol oxidase from *Escherichia coli*. *J. Am. Chem. Soc.* **2017**, *139*, 8346–8354. [CrossRef] [PubMed]
127. Borisov, V.B.; Gennis, R.B.; Hemp, J.; Verkhovsky, M.I. The cytochrome *bd* respiratory oxygen reductases. *Biochim. Biophys. Acta* **2011**, *1807*, 1398–1413. [CrossRef]
128. Arutyunyan, A.M.; Sakamoto, J.; Inadome, M.; Kabashima, Y.; Borisov, V.B. Optical and magneto-optical activity of cytochrome *bd* from *Geobacillus thermodenitrificans*. *Biochim. Biophys. Acta* **2012**, *1817*, 2087–2094. [CrossRef] [PubMed]

129. Murali, R.; Gennis, R.B.; Hemp, J. Evolution of the cytochrome *bd* oxygen reductase superfamily and the function of CydAA' in Archaea. *ISME J.* **2021**. [CrossRef]
130. Borisov, V.B. Cytochrome *bd*: Structure and properties. *Biochemistry* **1996**, *61*, 565–574.
131. Forte, E.; Borisov, V.B.; Vicente, J.B.; Giuffre, A. Cytochrome *bd* and gaseous ligands in bacterial physiology. *Adv. Microb. Physiol.* **2017**, *71*, 171–234. [CrossRef] [PubMed]
132. Borisov, V.B. Effect of membrane environment on ligand-binding properties of the terminal oxidase cytochrome *bd*-I from *Escherichia coli*. *Biochemistry* **2020**, *85*, 1603–1612. [CrossRef] [PubMed]
133. Borisov, V.B.; Siletsky, S.A.; Paiardini, A.; Hoogewijs, D.; Forte, E.; Giuffre, A.; Poole, R.K. Bacterial oxidases of the cytochrome *bd* family: Redox enzymes of unique structure, function and utility as drug targets. *Antioxid. Redox Signal.* **2021**, *34*, 1280–1318. [CrossRef] [PubMed]
134. Hill, J.J.; Alben, J.O.; Gennis, R.B. Spectroscopic evidence for a heme-heme binuclear center in the cytochrome *bd* ubiquinol oxidase from *Escherichia coli*. *Proc. Natl. Acad. Sci. USA* **1993**, *90*, 5863–5867. [CrossRef] [PubMed]
135. Tsubaki, M.; Hori, H.; Mogi, T.; Anraku, Y. Cyanide-binding site of *bd*-type ubiquinol oxidase from *Escherichia coli*. *J. Biol. Chem.* **1995**, *270*, 28565–28569. [CrossRef]
136. Borisov, V.; Arutyunyan, A.M.; Osborne, J.P.; Gennis, R.B.; Konstantinov, A.A. Magnetic circular dichroism used to examine the interaction of *Escherichia coli* cytochrome *bd* with ligands. *Biochemistry* **1999**, *38*, 740–750. [CrossRef]
137. Vos, M.H.; Borisov, V.B.; Liebl, U.; Martin, J.L.; Konstantinov, A.A. Femtosecond resolution of ligand-heme interactions in the high-affinity quinol oxidase *bd*: A di-heme active site? *Proc. Natl. Acad. Sci. USA* **2000**, *97*, 1554–1559. [CrossRef]
138. Borisov, V.B.; Sedelnikova, S.E.; Poole, R.K.; Konstantinov, A.A. Interaction of cytochrome *bd* with carbon monoxide at low and room temperatures: Evidence that only a small fraction of heme b_{595} reacts with CO. *J. Biol. Chem.* **2001**, *276*, 22095–22099. [CrossRef]
139. Borisov, V.B.; Liebl, U.; Rappaport, F.; Martin, J.L.; Zhang, J.; Gennis, R.B.; Konstantinov, A.A.; Vos, M.H. Interactions between heme *d* and heme b_{595} in quinol oxidase *bd* from *Escherichia coli*: A photoselection study using femtosecond spectroscopy. *Biochemistry* **2002**, *41*, 1654–1662. [CrossRef]
140. Arutyunyan, A.M.; Borisov, V.B.; Novoderezhkin, V.I.; Ghaim, J.; Zhang, J.; Gennis, R.B.; Konstantinov, A.A. Strong excitonic interactions in the oxygen-reducing site of *bd*-type oxidase: The Fe-to-Fe distance between hemes *d* and b_{595} is 10 A. *Biochemistry* **2008**, *47*, 1752–1759. [CrossRef]
141. Borisov, V.B. Interaction of *bd*-type quinol oxidase from *Escherichia coli* and carbon monoxide: Heme *d* binds CO with high affinity. *Biochemistry* **2008**, *73*, 14–22. [CrossRef] [PubMed]
142. Bloch, D.A.; Borisov, V.B.; Mogi, T.; Verkhovsky, M.I. Heme/heme redox interaction and resolution of individual optical absorption spectra of the hemes in cytochrome *bd* from *Escherichia coli*. *Biochim. Biophys. Acta* **2009**, *1787*, 1246–1253. [CrossRef]
143. Rappaport, F.; Zhang, J.; Vos, M.H.; Gennis, R.B.; Borisov, V.B. Heme-heme and heme-ligand interactions in the di-heme oxygen-reducing site of cytochrome *bd* from *Escherichia coli* revealed by nanosecond absorption spectroscopy. *Biochim. Biophys. Acta* **2010**, *1797*, 1657–1664. [CrossRef] [PubMed]
144. Borisov, V.B.; Verkhovsky, M.I. Accommodation of CO in the di-heme active site of cytochrome *bd* terminal oxidase from *Escherichia coli*. *J. Inorg. Biochem.* **2013**, *118*, 65–67. [CrossRef] [PubMed]
145. Siletsky, S.A.; Zaspa, A.A.; Poole, R.K.; Borisov, V.B. Microsecond time-resolved absorption spectroscopy used to study CO compounds of cytochrome *bd* from *Escherichia coli*. *PLoS ONE* **2014**, *9*, e95617. [CrossRef]
146. Siletsky, S.A.; Rappaport, F.; Poole, R.K.; Borisov, V.B. Evidence for fast electron transfer between the high-spin haems in cytochrome *bd*-I from *Escherichia coli*. *PLoS ONE* **2016**, *11*, e0155186. [CrossRef]
147. Siletsky, S.A.; Dyuba, A.V.; Elkina, D.A.; Monakhova, M.V.; Borisov, V.B. Spectral-kinetic analysis of recombination reaction of heme centers of *bd*-type quinol oxidase from *Escherichia coli* with carbon monoxide. *Biochemistry* **2017**, *82*, 1354–1366. [CrossRef]
148. Svensson, M.; Nilsson, T. Flow-flash study of the reaction between cytochrome *bo* and oxygen. *Biochemistry* **1993**, *32*, 5442–5447. [CrossRef]
149. Borisov, V.B.; Smirnova, I.A.; Krasnosel'skaya, I.A.; Konstantinov, A.A. Oxygenated cytochrome *bd* from *Escherichia coli* can be converted into the oxidized form by lipophilic electron acceptors. *Biochemistry* **1994**, *59*, 437–443.
150. D'Mello, R.; Hill, S.; Poole, R.K. The oxygen affinity of cytochrome *bo*′ in *Escherichia coli* determined by the deoxygenation of oxyleghemoglobin and oxymyoglobin: K_m values for oxygen are in the submicromolar range. *J. Bacteriol.* **1995**, *177*, 867–870. [CrossRef]
151. D'mello, R.; Hill, S.; Poole, R.K. The cytochrome *bd* quinol oxidase in *Escherichia coli* has an extremely high oxygen affinity and two-oxygen-binding haems: Implicaitons for regulation of activity in vivo by oxygen inihibition. *Microbiology* **1996**, *142*, 755–763. [CrossRef]
152. Belevich, I.; Borisov, V.B.; Konstantinov, A.A.; Verkhovsky, M.I. Oxygenated complex of cytochrome *bd* from *Escherichia coli*: Stability and photolability. *FEBS Lett.* **2005**, *579*, 4567–4570. [CrossRef] [PubMed]
153. Belevich, I.; Borisov, V.B.; Bloch, D.A.; Konstantinov, A.A.; Verkhovsky, M.I. Cytochrome *bd* from *Azotobacter vinelandii*: Evidence for high-affinity oxygen binding. *Biochemistry* **2007**, *46*, 11177–11184. [CrossRef]
154. Cotter, P.A.; Chepuri, V.; Gennis, R.B.; Gunsalus, R.P. Cytochrome *o* (*cyoABCDE*) and *d* (*cydAB*) oxidase gene expression in *Escherichia coli* is regulated by oxygen, pH, and the *fnr* gene product. *J. Bacteriol.* **1990**, *172*, 6333–6338. [CrossRef]

155. Alexeeva, S.; Hellingwerf, K.; Teixeira de Mattos, M.J. Quantitative assessment of oxygen availability: Perceived aerobiosis and its effect on flux distribution in the respiratory chain of *Escherichia coli*. *J. Bacteriol.* **2002**, *184*, 1402–1406. [CrossRef]
156. Rolfe, M.D.; Ter Beek, A.; Graham, A.I.; Trotter, E.W.; Asif, H.M.; Sanguinetti, G.; de Mattos, J.T.; Poole, R.K.; Green, J. Transcript profiling and inference of *Escherichia coli* K-12 ArcA activity across the range of physiologically relevant oxygen concentrations. *J. Biol. Chem.* **2011**, *286*, 10147–10154. [CrossRef]
157. Ederer, M.; Steinsiek, S.; Stagge, S.; Rolfe, M.D.; Ter Beek, A.; Knies, D.; Teixeira de Mattos, M.J.; Sauter, T.; Green, J.; Poole, R.K.; et al. A mathematical model of metabolism and regulation provides a systems-level view of how *Escherichia coli* responds to oxygen. *Front. Microbiol.* **2014**, *5*, 124. [CrossRef] [PubMed]
158. Bettenbrock, K.; Bai, H.; Ederer, M.; Green, J.; Hellingwerf, K.J.; Holcombe, M.; Kunz, S.; Rolfe, M.D.; Sanguinetti, G.; Sawodny, O.; et al. Towards a systems level understanding of the oxygen response of *Escherichia coli*. *Adv. Microb. Physiol.* **2014**, *64*, 65–114. [CrossRef] [PubMed]
159. Forte, E.; Borisov, V.B.; Konstantinov, A.A.; Brunori, M.; Giuffre, A.; Sarti, P. Cytochrome *bd*, a key oxidase in bacterial survival and tolerance to nitrosative stress. *Ital. J. Biochem.* **2007**, *56*, 265–269.
160. Borisov, V.B.; Forte, E.; Siletsky, S.A.; Arese, M.; Davletshin, A.I.; Sarti, P.; Giuffre, A. Cytochrome *bd* protects bacteria against oxidative and nitrosative stress: A potential target for next-generation antimicrobial agents. *Biochemistry* **2015**, *80*, 565–575. [CrossRef]
161. Giuffre, A.; Borisov, V.B.; Mastronicola, D.; Sarti, P.; Forte, E. Cytochrome *bd* oxidase and nitric oxide: From reaction mechanisms to bacterial physiology. *FEBS Lett.* **2012**, *586*, 622–629. [CrossRef] [PubMed]
162. Giuffre, A.; Borisov, V.B.; Arese, M.; Sarti, P.; Forte, E. Cytochrome *bd* oxidase and bacterial tolerance to oxidative and nitrosative stress. *Biochim. Biophys. Acta* **2014**, *1837*, 1178–1187. [CrossRef] [PubMed]
163. Forte, E.; Borisov, V.B.; Siletsky, S.A.; Petrosino, M.; Giuffre, A. In the respiratory chain of *Escherichia coli* cytochromes *bd*-I and *bd*-II are more sensitive to carbon monoxide inhibition than cytochrome bo_3. *Biochim. Biophys. Acta Bioenerg.* **2019**, *1860*, 148088. [CrossRef]
164. Borisov, V.B.; Forte, E.; Konstantinov, A.A.; Poole, R.K.; Sarti, P.; Giuffre, A. Interaction of the bacterial terminal oxidase cytochrome *bd* with nitric oxide. *FEBS Lett.* **2004**, *576*, 201–204. [CrossRef] [PubMed]
165. Borisov, V.B.; Forte, E.; Sarti, P.; Brunori, M.; Konstantinov, A.A.; Giuffre, A. Nitric oxide reacts with the ferryl-oxo catalytic intermediate of the Cu_B-lacking cytochrome *bd* terminal oxidase. *FEBS Lett.* **2006**, *580*, 4823–4826. [CrossRef] [PubMed]
166. Borisov, V.B.; Forte, E.; Sarti, P.; Brunori, M.; Konstantinov, A.A.; Giuffre, A. Redox control of fast ligand dissociation from *Escherichia coli* cytochrome *bd*. *Biochem. Biophys. Res. Commun.* **2007**, *355*, 97–102. [CrossRef]
167. Mason, M.G.; Shepherd, M.; Nicholls, P.; Dobbin, P.S.; Dodsworth, K.S.; Poole, R.K.; Cooper, C.E. Cytochrome *bd* confers nitric oxide resistance to *Escherichia coli*. *Nat. Chem. Biol.* **2009**, *5*, 94–96. [CrossRef] [PubMed]
168. Borisov, V.B.; Forte, E.; Giuffre, A.; Konstantinov, A.; Sarti, P. Reaction of nitric oxide with the oxidized di-heme and heme-copper oxygen-reducing centers of terminal oxidases: Different reaction pathways and end-products. *J. Inorg. Biochem.* **2009**, *103*, 1185–1187. [CrossRef]
169. Shepherd, M.; Achard, M.E.; Idris, A.; Totsika, M.; Phan, M.D.; Peters, K.M.; Sarkar, S.; Ribeiro, C.A.; Holyoake, L.V.; Ladakis, D.; et al. The cytochrome *bd*-I respiratory oxidase augments survival of multidrug-resistant *Escherichia coli* during infection. *Sci. Rep.* **2016**, *6*, 35285. [CrossRef]
170. Holyoake, L.V.; Hunt, S.; Sanguinetti, G.; Cook, G.M.; Howard, M.J.; Rowe, M.L.; Poole, R.K.; Shepherd, M. CydDC-mediated reductant export in *Escherichia coli* controls the transcriptional wiring of energy metabolism and combats nitrosative stress. *Biochem. J.* **2016**, *473*, 693–701. [CrossRef]
171. Jones-Carson, J.; Husain, M.; Liu, L.; Orlicky, D.J.; Vazquez-Torres, A. Cytochrome *bd*-dependent bioenergetics and antinitrosative defenses in *Salmonella* pathogenesis. *mBio* **2016**, *7*, e02052-16. [CrossRef] [PubMed]
172. Meng, Q.; Yin, J.; Jin, M.; Gao, H. Distinct nitrite and nitric oxide physiologies in *Escherichia coli* and *Shewanella oneidensis*. *Appl. Environ. Microbiol.* **2018**, *84*, e00559-18. [CrossRef] [PubMed]
173. Beebout, C.J.; Eberly, A.R.; Werby, S.H.; Reasoner, S.A.; Brannon, J.R.; De, S.; Fitzgerald, M.J.; Huggins, M.M.; Clayton, D.B.; Cegelski, L.; et al. Respiratory heterogeneity shapes biofilm formation and host colonization in uropathogenic *Escherichia coli*. *mBio* **2019**, *10*, e02400-18. [CrossRef] [PubMed]
174. Borisov, V.B.; Forte, E.; Siletsky, S.A.; Sarti, P.; Giuffre, A. Cytochrome *bd* from *Escherichia coli* catalyzes peroxynitrite decomposition. *Biochim. Biophys. Acta* **2015**, *1847*, 182–188. [CrossRef] [PubMed]
175. Borisov, V.; Gennis, R.; Konstantinov, A.A. Peroxide complex of cytochrome *bd*: Kinetics of generation and stability. *Biochem. Mol. Biol. Int.* **1995**, *37*, 975–982.
176. Borisov, V.B.; Gennis, R.B.; Konstantinov, A.A. Interaction of cytochrome *bd* from *Escherichia coli* with hydrogen peroxide. *Biochemistry* **1995**, *60*, 231–239.
177. Borisov, V.B.; Davletshin, A.I.; Konstantinov, A.A. Peroxidase activity of cytochrome *bd* from *Escherichia coli*. *Biochemistry* **2010**, *75*, 428–436. [CrossRef]
178. Borisov, V.B.; Forte, E.; Davletshin, A.; Mastronicola, D.; Sarti, P.; Giuffre, A. Cytochrome *bd* oxidase from *Escherichia coli* displays high catalase activity: An additional defense against oxidative stress. *FEBS Lett.* **2013**, *587*, 2214–2218. [CrossRef]
179. Forte, E.; Borisov, V.B.; Davletshin, A.; Mastronicola, D.; Sarti, P.; Giuffre, A. Cytochrome *bd* oxidase and hydrogen peroxide resistance in *Mycobacterium tuberculosis*. *mBio* **2013**, *4*, e01006-13. [CrossRef]

180. Al-Attar, S.; Yu, Y.; Pinkse, M.; Hoeser, J.; Friedrich, T.; Bald, D.; de Vries, S. Cytochrome *bd* displays significant quinol peroxidase activity. *Sci. Rep.* **2016**, *6*, 27631. [CrossRef]
181. Kita, K.; Konishi, K.; Anraku, Y. Terminal oxidases of *Escherichia coli* aerobic respiratory chain. II. Purification and properties of cytochrome b_{558}-*d* complex from cells grown with limited oxygen and evidence of branched electron-carrying systems. *J. Biol. Chem.* **1984**, *259*, 3375–3381. [CrossRef]
182. Sakamoto, J.; Koga, E.; Mizuta, T.; Sato, C.; Noguchi, S.; Sone, N. Gene structure and quinol oxidase activity of a cytochrome *bd*-type oxidase from *Bacillus stearothermophilus*. *Biochim. Biophys. Acta* **1999**, *1411*, 147–158. [CrossRef]
183. Forte, E.; Siletsky, S.A.; Borisov, V.B. In *Escherichia coli* ammonia inhibits cytochrome bo_3 but activates cytochrome *bd*-I. *Antioxidants* **2021**, *10*, 13. [CrossRef] [PubMed]
184. Mascolo, L.; Bald, D. Cytochrome *bd* in *Mycobacterium tuberculosis*: A respiratory chain protein involved in the defense against antibacterials. *Prog. Biophys. Mol. Biol.* **2020**, *152*, 55–63. [CrossRef] [PubMed]
185. Lee, B.S.; Sviriaeva, E.; Pethe, K. Targeting the cytochrome oxidases for drug development in mycobacteria. *Prog. Biophys. Mol. Biol.* **2020**, *152*, 45–54. [CrossRef]
186. Cook, G.M.; Hards, K.; Dunn, E.; Heikal, A.; Nakatani, Y.; Greening, C.; Crick, D.C.; Fontes, F.L.; Pethe, K.; Hasenoehrl, E.; et al. Oxidative phosphorylation as a target space for tuberculosis: Success, caution, and future directions. *Microbiol. Spectr.* **2017**, *5*. [CrossRef]
187. Bald, D.; Villellas, C.; Lu, P.; Koul, A. Targeting energy metabolism in *Mycobacterium tuberculosis*, a new paradigm in antimycobacterial drug discovery. *mBio* **2017**, *8*, e00272-17. [CrossRef]
188. Hards, K.; Cook, G.M. Targeting bacterial energetics to produce new antimicrobials. *Drug Resist. Updat.* **2018**, *36*, 1–12. [CrossRef]
189. Winstedt, L.; Frankenberg, L.; Hederstedt, L.; von Wachenfeldt, C. *Enterococcus faecalis* V583 contains a cytochrome *bd*-type respiratory oxidase. *J. Bacteriol.* **2000**, *182*, 3863–3866. [CrossRef]
190. Lee, B.S.; Hards, K.; Engelhart, C.A.; Hasenoehrl, E.J.; Kalia, N.P.; Mackenzie, J.S.; Sviriaeva, E.; Chong, S.M.S.; Manimekalai, M.S.S.; Koh, V.H.; et al. Dual inhibition of the terminal oxidases eradicates antibiotic-tolerant *Mycobacterium tuberculosis*. *EMBO Mol. Med.* **2021**, *13*, e13207. [CrossRef]
191. Saini, V.; Chinta, K.C.; Reddy, V.P.; Glasgow, J.N.; Stein, A.; Lamprecht, D.A.; Rahman, M.A.; Mackenzie, J.S.; Truebody, B.E.; Adamson, J.H.; et al. Hydrogen sulfide stimulates *Mycobacterium tuberculosis* respiration, growth and pathogenesis. *Nat. Commun.* **2020**, *11*, 557. [CrossRef] [PubMed]
192. Kunota, T.T.R.; Rahman, M.A.; Truebody, B.E.; Mackenzie, J.S.; Saini, V.; Lamprecht, D.A.; Adamson, J.H.; Sevalkar, R.R.; Lancaster, J.R., Jr.; Berney, M.; et al. *Mycobacterium tuberculosis* H_2S functions as a sink to modulate central metabolism, bioenergetics, and drug susceptibility. *Antioxidants* **2021**, *10*, 1285. [CrossRef] [PubMed]